creative commons
COMMONS DEED

저작자표시-비영리-변경금지 2.0 대한민국

이용자는 아래의 조건을 따르는 경우에 한하여 자유롭게

- 이 저작물을 복제, 배포, 전송, 전시, 공연 및 방송할 수 있습니다.

다음과 같은 조건을 따라야 합니다:

저작자표시. 귀하는 원저작자를 표시하여야 합니다.

비영리. 귀하는 이 저작물을 영리 목적으로 이용할 수 없습니다.

변경금지. 귀하는 이 저작물을 개작, 변형 또는 가공할 수 없습니다.

- 귀하는, 이 저작물의 재이용이나 배포의 경우, 이 저작물에 적용된 이용허락조건을 명확하게 나타내어야 합니다.
- 저작권자로부터 별도의 허가를 받으면 이러한 조건들은 적용되지 않습니다.

저작권법에 따른 이용자의 권리는 위의 내용에 의하여 영향을 받지 않습니다.

이것은 이용허락규약(Legal Code)을 이해하기 쉽게 요약한 것입니다.

Disclaimer

dCollection

연세대학교
YONSEI UNIVERSITY

Visualization of the Biologic Factors in Bone Metabolism of Osteoporosis using Modified Bone Clearing Technique

Byung-Ho Jin

Department of Medicine

The Graduate School, Yonsei University

연세대학교
YONSEI UNIVERSITY

Visualization of the Biologic Factors in Bone Metabolism of Osteoporosis using Modified Bone Clearing Technique

Directed by Professor Yong Eun Cho

The Doctoral Dissertation
submitted to the Department of Medicine,
the Graduate School of Yonsei University
in partial fulfillment of the requirements for the degree
of Doctor of Philosophy in Medical Science

Byung-Ho Jin

December 2021

연세대학교
YONSEI UNIVERSITY

This certifies that the Doctoral Dissertation of Byung-Ho Jin is approved.

Thesis Supervisor : Yong Eun Cho

Thesis Committee Member#1 : Sung Uk Kuh

Thesis Committee Member#2 : Inbo Han

Thesis Committee Member#3: Shin Ae Kang

Thesis Committee Member#4: Jeong Yoon Park

The Graduate School
Yonsei University

December 2021

연세대학교
YONSEI UNIVERSITY

ACKNOWLEDGEMENTS

I would like to express my thanks to the all people who gave me the opportunity to complete this thesis.

First of all, I am deeply grateful to my supervisor, professer Yong Eun Cho and Sung UK Kuh for detailed guidance and critical comments during the fulfillment of this dissertation. Special thanks go to professor In Bo Han for generous guidance and helpful advice at spine department on Cha medical school

Especially, I would like to express my sincere thanks to my parents and wife who constantly provide emotional support and took care of me in my aspects. This work may not have been completed without their support and encouragement.

It was great accomplishment of mine that I could broaden my academic knowledge and upgrade my experimental skill while completing the thesis. Based on it, I would like to contribute to the advance of the understanding of molecular patterns and cellular circuits in various biological tissues in the three dimensional spaces.

연세대학교
YONSEI UNIVERSITY

<TABLE OF CONTENTS>

연세대학교
YONSEI UNIVERSITY

연세대학교
YONSEI UNIVERSITY

LIST OF FIGURES

연세대학교
YONSEI UNIVERSITY

연세대학교
YONSEI UNIVERSITY

ABSTRACT

Visualization of the Biologic Factors in Bone Metabolism of Osteoporosis using Modified Bone Clearing Technique

Byung-Ho Jin

Department of Medicine
The Graduate School, Yonsei University

(Directed by Professor Yong Eun Cho)

Recent developments in tissue clearing methods, such as the passive clearing technique (PACT), have allowed three-dimensional analysis of biological structures in whole, intact tissues, thereby providing a greater understanding of spatial relationships and biological circuits. Nonetheless, issues remain in maintaining structural integrity and preventing tissue expansion/shrinkage with rapid clearing and prevent the wide application of these techniques to hard bone tissues, such as the femur and tibia. Here, we present an optimized psPACT-based bone clearing method, Bone-mPACT+, that incorporates Calci-mPACT+ and 20EDTA-mPACT+ to improve bone tissue clearing efficiency without sacrificing optical transparency. We also present a further modified Bone-mPACT+ Advance protocol specifically optimized for processing the largest and hardest rat bones for easy clearing and imaging using established tissue clearing methods. We provide proof-of-concept support for our optimized protocol by investigating the endogenous fluorescence and the expression of RUNX2, OPG, RANKL, and the relatively understudied PRDM10 and PRDM12 in maternal mouse bones during pregnancy and in bones of male osteoporosis model rats following orchiectomy. Our observation of OPG, RANKL, PRDM10, and PRDM12 expression in the transparent bone during osteoporosis development suggests potential roles of these genes that could guide future functional studies of metabolic and degenerative bone diseases.

Key words : transparent bone, bone clearing, passive clearing technique, Bone-mPACT+, osteoporosis.

연세대학교
YONSEI UNIVERSITY

Visualization of the Biologic Factors in Bone Metabolism of Osteoporosis using Modified Bone Clearing Technique

Byung-Ho Jin

Department of Medicine
The Graduate School, Yonsei University

(Directed by Professor Yong Eun Cho)

I. INTRODUCTION

Significant recent advancements in the field of tissue clearing have increased the appreciation of molecular patterns and cellular circuits in various biological tissues in three-dimensional space. As opposed to traditional immunohistochemistry in frozen or paraffin sections, clear lipid-exchanged acrylamide-hybridized rigid imaging/immunostaining/in situ-hybridization-compatible tissue-hydrogel (CLARITY)-based methods enable microscopy studies of tissue architecture in intact whole tissues and organs[1,2]. We recently reported the development of novel passive tissue clearing techniques (PACTs), process-separate PACT (psPACT) and modified PACT (mPACT that significantly reduces required tissue processing times while improving achieved optical transparency)[3-5].

A full understanding of the biological processes that shape a degenerating bone requires the study of these processes across time and, when possible, across three-dimensional space. However, processing hard bones via CLARITY-based methods has proven challenging because hard bone tissues require long clearing times, even with the harsh treatments used in the majority of tissue clearing protocols. Some studies have sought to address this issue, but the currently published methods specific for clearing vertebrate bones are

연세대학교
YONSEI UNIVERSITY

limited by either their long processing times[6] or the use of organic solvents[7], which are known to produce artifacts in subsequent immunostaining.

Here, we present an optimized version of our previously published mPACT method that is specifically geared towards clearing rodent bones. The protocol, which we refer to as Bone-mPACT+ (consisting of the 20EDTA-mPACT+ and Calci-mPACT+ protocols), maintains tissue integrity without compromising the achieved optical transparency. We also present Bone-mPACT+ Advance, which allows clearing of thin sections of rat hard bones. The Bone-mPACT+ Advance protocol addresses the limitations imposed by the narrow 2 mm working distance of traditional confocal microscopes, which currently prevents the study of samples larger than rat bones.

The receptor activator of nuclear factor κB ligand (RANKL; osteoclast differentiation factor), its natural receptor (RANK) and osteoprotegerin (OPG; osteoclastogenesis inhibitory factor), all belong to the family of tumor necrosis factors (TNF)[8,9]. RANKL is a protein expressed by osteoblasts and their precursors under the control of hormones, cytokines and proresorptive growth factors. RANKL is released by bone-forming osteoblasts and stimulates RANK on the surface of stem cells to form osteoclasts that mediate bone resorption. Osteoprotegerin is a natural inhibitor of RANKL and mice that are deficient in osteoprotegerin exhibit osteoporosis, whereas mice that over-express osteoprotegerin show reduced numbers of osteoclasts and high bone mass[10].

The present study is a proof-of-concept investigation of bone metabolism during pregnancy and in a rat model of male osteoporosis via Calci-mPACT+, and with imaging of endogenous fluorescence. We also investigated the expression of osteoprotegerin and RANKL, in these two rodent degenerative hard bone models after clearing with Bone-mPACT+ (20EDTA-mPACT) and Bone-mPACT Advance with 20% EDTA.

We also investigated the expression of PR domain 10 (PRDM10) and PRDM12 of the PRDM (PRDI-BF1 and RIZ homology domain-containing) family.

연세대학교
YONSEI UNIVERSITY

PRDMs have emerged as important transcriptional regulators that control the development of numerous organ systems throughout embryogenesis[11-14]. While both PRDM10 and PRDM12 have been implicated in key developmental processes, such as cell fate specification, and in various cancer, they remain significantly less well characterized than other PRDM family members. Our studies demonstrate the applicability and efficacy of the Bone-mPACT+ methods for clearing hard bone tissue, and they provide the first three-dimensional survey of PRDM10 and PRDM12 expression in the degenerative bone tissues.

연세대학교
YONSEI UNIVERSITY

II. MATERIALS AND METHODS

1. Animals

All experimental procedures were carried out in strict accordance with the recommendations provided by the Ministry of Agriculture, Food, and Rural Affairs (MAFRA) and were approved by the Institutional Animal Care and Use Committee (IACUC) at Yonsei University (licenses #2017-0230 and #2015-0147).

Adult male and female Institute of Cancer Research (ICR) mice were purchased from Orient Inc. (Gyeonggi-do, Korea) and were raised in a specific pathogen-free (SPF) environment. Mouse embryos were isolated from embryonic day 13.5 (E13.5) to E17.5. Bones from pregnant female mice were isolated from E13.5 to E17.5 (i.e., gestational days 13.5 and 17.5). Nine-week-old male SD (Sprague-Dawley) rats were purchased from Central Lab Animal Inc. (Seoul, Korea), and acclimated separately in pathogen-free ventilated cages with a controlled environment (temperature 22±4℃, humidity 65±5%, day-night cycle 06:00–18:00). The rats were permitted free intake of tap water and standard rodent chow (SAFE, Augy, France) containing 8 g/kg calcium, 4.2 g/kg phosphorus, and 1000 UI/kg vitamin D3.

Male rats were orchiectomized to induce male osteoporosis, and a few control rats underwent a sham operation. All rats in the orchiectomy group underwent bilateral orchiectomy. Those in the sham surgery (sham) group underwent the same procedure, except that the testes were merely identified, not removed. At postoperative date (POD) 8 weeks, orchiectomized rats were sacrificed using CO2 inhalation, and their femurs and lumbar spines were removed. Each sample was transferred to sufficient 4% paraformaldehyde (PFA) solution to cover the tissue in a 50 mL tube and stored at 4 °C for 24 hours.

2. Orchiectomy and sham operation procedure

연세대학교
YONSEI UNIVERSITY

Anesthesia was induced with 5% isoflurane, and Rompun (2.5 mg/kg, Bayer Korea, Seoul, Korea) and Zoletil (5 mg/kg, Virbac Korea, Seoul, Korea) were then injected intraperitoneally for generalized anesthesia. Anesthesia was maintained by the administration of 2.5% isoflurane and oxygen via a coaxial nose cone.

Bilateral orchiectomy was performed via a scrotal approach. The anesthetized rat was placed supine on the operating table, and its position was fixed using adhesive tape. The scrotal hair was bilaterally shaved, and betadine preparation was applied as an aseptic maneuver. If the cremaster muscle was stimulated during the betadine preparation, resulting in ascension of the testes, a downward stroke was performed to lower the testes back into place. A small 1.0-cm median incision was made through the skin at the tip of the scrotum. The cremaster muscles were opened with an incision. At the entrance to the scrotal cavity, the testicular fat pad was located with the testis, followed by the caput epididymis, the vas deferens, and the testicular blood vessels, all of which were pulled through the incision using blunt forceps. After identifying the testis, a single ligature was placed on the spermatic cord around the vas deferens and the blood vessels. The testis and epididymis were removed. This procedure was repeated for the other testis and epididymis. The cremaster muscle and scrotal skin were sutured layer by layer. The same preparation was performed on animals in the sham operation group, allowing the authors to visually identify each testis, epididymis, vas deferens, and testicular blood vessels. After visual identification, the cremaster muscle and skin were sutured without ligation or resection of the testes or epididymis.

3. Isolation of mouse embryos, brain and bones

Upon opening the mouse thorax, an incision was made to the right atrium of the heart. Mice were then perfused with equal volumes of cold 0.1 M phosphate-buffered saline (PBS) with 10 unit/mL heparin and 4% PFA.

연세대학교
YONSEI UNIVERSITY

Embryos and bones were then isolated using methods described previously[5,24]. Each sample was transferred to sufficient 4% PFA solution to cover the tissue in a 50 mL tube and stored at 4 °C for 24 hours.

4. psPACT and mPACT of mouse brain and embryos

Each fixed sample was washed for 1 hour with 0.1 M phosphate-buffered saline (PBS) in a 50 mL tube and then transferred to sufficient 4% acrylamide (AA; Sigma-Aldrich, Inc., MO, USA) in 0.1 M PBS to cover the sample in a 50 mL tube at 37 °C. After 24 hours, the sample was covered with 0.25% 2,2′-Azobis[2-(2-imidazolin-2-yl)propane]dihydrochloride (VA-044, Wako Chemicals USA, Inc., VA, USA) photoinitiator in 0.1 M PBS in a 50 mL tube at 37°C for 6 h. The samples for psPACT and mPACT were embedded under vacuum and nitrogen gas for 10 min each. The tissue was transferred to a 50 mL tube containing sufficient clearing solutions: 8S (8% sodium dodecyl sulfate (Affymetrix, OH, USA) in 0.1 M PBS, pH 8.0), 10C (10% sodium deoxycholate (Wako Chemicals USA, Inc., VA, USA) in 0.1 M PBS, pH 8.0), 8S10C (8% SDS and 10% SDC in 0.1 M PBS, pH 8.0) and 4S5C (4% SDS and 5% SDC in 0.1 M PBS, pH 8.0) with 0.5% α-thioglycerol (+; Sigma-Aldrich, Inc., MO, USA). The sample was then incubated with shaking at 150 rpm at 37–45 °C until the tissue cleared.

5. Bone-mPACT+

Each bone sample was submerged in 4% PFA and stored at 4 °C for 24 hours. Samples for Calci-mPACT+ testing were washed with PBST (0.1 M PBS plus 0.1% Triton X-100; Sigma-Aldrich, Inc., MO, USA) and then submerged in Calci-Clear Rapid decalcification solution (National Diagnostics, GA, USA) at 45 °C for 6–12 hours (mice: 6 hours, rats: 12 hours). Samples for 20EDTA-mPACT+ testing were submerged in a decalcification solution of 20% ethylene-diamine-tetraacetic acid (EDTA; Sigma-Aldrich, Inc., MO, USA) in

연세대학교
YONSEI UNIVERSITY

0.1 M PBS at 45 °C for 3–8 days (mice: 3 days, rats: 7 days). After a 1 hour wash in PBST, samples were submerged in 4% acrylamide in 0.1 M PBS at 45 °C for 6–8 hours, followed by incubation in 0.25% VA-044 in 0.1 M PBS at 37 °C for 6–8 hours. Samples were embedded under vacuum and nitrogen gas for 10 min each. Samples processed with the Bone-mPACT+ protocol were removed from the embedded hydrogel and transferred to 8S10C+ clearing solution with 0.5% α-thioglycerol in a shaking incubator at 45 °C and 150 rpm until optical transparency was achieved. Sample were or 25% triethanolamine (TEA; Daejung Chemicals & Metals Co., Ltd., Gyeonggi-do, Republic of Korea) at 45 °C for 2 days. Samples were washed with PBST and then incubated in nRIMS solution at room temperature for 1–2 days. For more details, see **Figure 1**.

6. Bone-mPACT+ Advance

After the embedding process of Bone-mPACT+, the sample was sagittal slicing with a blade or Vibratome (VT-1000-S; Leica biosystems, Wetzlar, Germany). The sample was gently shaken and incubated at room temperature for 30 min with 20 mL of AD1 solution in a 50 mL tube. The sample was transferred to a 50 mL tube containing sufficient AD2 in 0.1 M PBS, and the sample was gently shaken and incubated at room temperature for 10 min. The sample was transferred to a coverslip and overlaid with a coverslip. After drying for 30 min, the sample was transferred to a 50 mL tube containing sufficient 8S10C+ clearing solution with 0.5% α-thioglycerol. The sample was then incubated with shaking at 150 rpm for 45 °C until the tissue cleared. All samples were washed with 0.1 M PBST and submerged in 25% triethanolamine at 45 °C for 2 days. Sample were washed with PBST and then incubated in nRIMS solution at room temperature for 1–2 days (For more detailed instructions, see also **Figures 1 and 8A**).

연세대학교
YONSEI UNIVERSITY

7. CUBIC

After fixation in 4% PFA, samples were immersed in CUBIC-L solution (Tokyo Chemical Industry Co., Ltd., Tokyo, Japan) at 37 °C for 4 days in a shaking incubator. Samples were washed in 0.1 M PBS for 24 h and incubated in CUBIC-B solution (Tokyo Chemical Industry Co., Ltd., Tokyo, Japan) at 37 °C for 5 days. Samples were washed in 0.1 M PBS at 37 °C for 24 hours and re-incubated in CUBIC-L solution for 3 days. Samples were washed in PBS for 24 hours and pre-treated in 50% CUBIC-R+ solution (Tokyo Chemical Industry Co., Ltd., Tokyo, Japan) at 37 °C for 1 day. Samples were then incubated in 100% CUBIC-R+ solution at 37 °C for 1 day.

8. PEGASOS

After fixation in 4% PFA, the samples were incubated in 20% EDTA in 0.1 M PBS at 37 °C for 4 days. Samples were incubated in decolorization solution for 48 hours at room temperature. Decolorization solution was prepared with 25% quadrol in 0.1 M PBS. Samples were then sequentially incubated in 30, 50, and 70% (*v/v*) tert-butanol (Daejung Chemicals & Metals Co., Ltd., Gyeonggi-do, Republic of Korea) in dH2O for 48 h, and subsequently dehydrated in 70% tert-butanol, 27% ethylene glycol, and 3% quadrol (tB-PEG solution) at room temperature for 48 hours. Processed samples were immersed in 75% benzyl benzoate (Sigma-Aldrich, Inc., MO, USA) and 25% ethylene glycol (Sigma-Aldrich, Inc., MO, USA) in 0.1 M PBS (BB-PEG solution) for 24 hours at room temperature until optical clearance was achieved.

9. Bone-CLARITY

Fixed samples were washed with 0.1 M PBS and then submerged in 10% EDTA solution at 4 °C for 2 weeks with gentle shaking. Samples were submerged in 4% acrylamide and 0.25% VA-044 in 0.1 M PBS (A4P0 solution) at 4 °C for 24 hours, followed by incubation in fresh A4P0 solution at 37 °C for

연세대학교
YONSEI UNIVERSITY

6 h. Samples were embedded under vacuum and nitrogen gas for 10 min each. Samples were removed from the embedded hydrogel and transferred to 8% SDS solution in a shaking incubator at 45 ℃ and 150 rpm for 5 days. Sample were washed for 2 days with 0.1 M PBS and submerged in 25% quadrol in 0.1 M PBS at 37 ℃ for 2 days. Sample were washed for 1 day with 0.1 M PBS and incubated in nRIMS solution at room temperature for 1 day.

10. Immunostaining and preparation for imaging

Cleared bones were incubated in PBST for 2 hours and then blocked with 2% bovine serum albumin (BSA; Sigma-Aldrich Inc., St. Louis, MO, USA) in PBST for 6 hours. The samples were incubated for 24–72 hours with the following primary antibodies: anti-OPG (1:1000; Santa Cruz Biotechnology Inc., TX, USA), anti-RANKL (1:1000; Santa Cruz Biotechnology Inc., TX, USA), anti-RUNX2 (1:1000; Santa Cruz Biotechnology Inc., TX, USA), PRDM10 (1:100; Biorbyt, Cambridge, United Kingdom) and PRDM12 (1:100; Biorbyt, Cambridge, United Kingdom). The samples were then washed three times in PBST for 24–48 hours each, followed by incubation with the secondary antibodies and lectin dye (Lycopersicon esculentum (Tomato) Lectin (LEL, TL), DyLight® 594; Vector Laboratories, CA, USA), in PBST for 24–72 hours. Secondary antibodies were purchased as conjugates with Alexa Fluor 488/647 (1:200; Life Technologies, Darmstadt, Germany), and mounted with *n*RIMS solution in 50 mL tubes.

The *n*RIMS solution was prepared by mixing 0.8 g/mL Nycodenz (Axis-Shield Density Gradient Media, Oslo, Norway) in 30 mL of base buffer (0.01% sodium azide (Sigma-Aldrich, Inc., MO, USA) and 0.1% Tween-20 (Sigma-Aldrich, Inc., MO, USA) in 0.1 M PBS, pH 7.5). The labeled sample was washed three times with PBST solution for 24–72 hours and stored in 5 mL *n*RIMS solution for 6–24 hours. The sample was incubated in *n*RIMS solution in a confocal dish, and covered with a 24 mm diameter coverslip. Whole bone samples in *n*RIMS

연세대학교
YONSEI UNIVERSITY

solution were sandwiched between two 24 × 60 mm coverslips and small 1 mm thick magnets.

11. Image processing

All clear images were captured using a digital camera (iPhone-X; Apple Inc., CA, USA) and a stereoscopic microscope (SMZ745T; Nikon, Tokyo, Japan). Confocal microscopy was performed with an LSM-780 confocal microscope (Carl Zeiss, Oberkochen, Germany) at 10× magnification (0.45 NA, 2.0 mm working distance) using the associated Zeiss software (ZEN 3.2 black edition; Carl Zeiss, Oberkochen, Germany). Three-dimensional images and videos were edited into serial images using Imaris v8.01 software (Bitplane, Belfast, United Kingdom).

12. Liquid viscosity test

All reagents were suctioned for 3 sec at room temperature using a 10 mL serological pipette (D-51588; Sarstedt, Inc., Nümbrecht, Germany) and a Pipet-Aid® pipette pump (4-000-100; Drummond Scientific, Broomall, PA, USA). The volume of suctioned liquid was determined in mL in a 10 mL pipette. The results are the averages of five independent tests with each new pipette.

13. Light transmittance measurements

Sagittal sections (1.5 mm thick) of mouse brains cleared with psPACT and different combinations of clearing reagents were used to generate 6 mm round brain tablets containing the prefrontal cortex and basal ganglia in a metal eyelet, and the RI was adjusted. Brain tablets were transferred to a 96-well dish, and a spectrometer (Molecular Devices, CA, USA) was used to measure light transmittance (%) at 600 nm (optical density). The results were analyzed with SoftMax Pro 5 software (Molecular Devices, CA, USA). An average of three measurements was calculated for each sample. The final transmittance (%) of

연세대학교
YONSEI UNIVERSITY

the sample was normalized to the transmittance of the blank values (*n*RIMS solutions).

연세대학교
YONSEI UNIVERSITY

III. RESULTS

1. Generation of transparent rodent bones using an optimized PACT-based bone tissue clearing method.

We investigated the expression pattern of osteoporosis effectors in intact bone tissues by first optimizing process-separate passive clearing technique (psPACT)-based protocols to ensure rapid bone clearing and increased transparency after clearing. The psPACT protocol provides rapid tissue clearing and separation of tissue embedding in a hydrogel containing 4% acrylamide (AA) and photoinitiator (0.25% VA-044). It involves incubation of tissue in 8% sodium dodecyl sulfate (SDS) clearing solutions and in a clearing solution of mPACT (modified PACT) consisting of 8% SDS with 0.25–0.5% α-thioglycerol (TG)[3-5]. psPACT and mPACT protocols conserve the unique sample form by separating the polymerization process and do not require removal of the embedded hydrogel from sample surface.

In this study, we optimized the PACT-based bone clearing method for three-dimensional visualization in transparent bone by a method we named “Bone-mPACT+”. This method is consists of two decalcification steps: one is 20% EDTA based mPACT clearing (20EDTA-mPACT+) and the other is Calci-Clear Rapid solution-based mPACT clearing (Calci-mPACT+). In the newly optimized Bone-mPACT+ procedure for bone tissue, clearing and incubation were performed at 45 °C rather than at the standard temperature of 37 °C. This protocol, which we refer to as Bone-mPACT+, yielded transparent, undamaged bone tissues with no tissue expansion or shrinkage for 10–13 days. Figure 1 provides a detailed outline of the steps required for Bone-mPACT+.

The previously reported Bone-CLARITY[6] and PACT-DeCAL[15] protocols provide successful bone clearing, as the most important issues are the decalcification of hard bone tissue and a decrease autofluorescence after clearing. Decalcification in the bone clearing protocol removes minerals from

연세대학교
YONSEI UNIVERSITY

the bone to create soft bone tissue and facilitates the permeation of embedding and clearing solutions into the bone tissue. The currently available bone clearing protocols use 10–20% ethylenediaminetetraacetic acid (EDTA) for decalcification, but EDTA decalcification takes a very long time (e.g., PEGASOS: 5 days at 37 °C, and Bone-CLARITY: 14 days at 4 °C)[6,7,15]. We reduced the decalcification times for hard mouse femur bone tissue by modifying the PACT-based bone clearing protocol (prototype Bone-mPACT) with Calci-Clear Rapid solution (**Figure 2A**). As shown in **Figure 2B**, mouse femur bone (femur, tibia-fibula, and foot) was rapidly decalcified in 6 hours with Bone-mPACT (Calci-mPACT; Calci-Clear decalcify + mPACT). Mouse hind limb samples were cleared with Bone-mPACT at 45 °C for 5 days with an 8% SDS + 0.5% α-thioglycerol (8S+) clearing solution. Mouse fore limb samples (scapula, humerus, radius-ulna, and hand) required 4 days until transparency in the 8S+ clearing solution (**Figure 2C**).

The samples in the prototype Bone-mPACT were rapidly cleared within 8 days, but we observed sample damage in the form shrinkage and swelling of the inner constructs (e.g., bone marrow). We Calci-Clear Rapid solution successfully decalcified mouse bones in 6 hours, thereby decreasing the total bone clearing time, but it considerably preserved or increased the autofluorescence in the bone marrow. A recent study showed that the heme-rich bone marrow creates an autofluorescence problem, but this issue can be reduced by heme removal with a 25% solution of quadrol (*N,N,N',N'*-tetrakis(2-hydroxypropyl) ethylenediamine), and amino alcohol, before refractive index matching[6,7,15].

N,N,N',N'-tetrakis(2-hydroxypropyl) ethylenediamine (Quadrol) has high viscosity at room temperature; therefore, the use of this liquid has the inevitable drawbacks of requiring incubation at >50 °C and the expense of using a specific amino alcohol. We found that possible for amino alcohol, such as 25% triethanolamine (TEA) for their ease of use and low cost, and we compared efficiency of removal autofluorescence (**Figure 3A and B**). Note that

연세대학교
YONSEI UNIVERSITY

triethanolamine (TEA) is incorporated at a 10% concentration in CUBIC-R+ solution used in the CUBIC protocol.

We generated the transparent rat thoracic vertebrae via a prototype Bone-mPACT and incubated the samples at 45 °C for 2 days in solutions containing triethanolamine (TEA) at 10–25%. The 25% TEA solution gave the highest optical transparency after refractive index matching in *n*RIMS (nycodenz-based refractive index matching solution) solution for 1 day (**Figure 3C**). Mouse femur bones were incubated in Bone-mPACT for 2 days in 25% quadrol and 25% triethanolamine (TEA). Both bone samples showed increased optical transparency to the naked eye when incubated in *n*RIMS solution for 1 day and compared with samples not treated with an amino alcohol (**Figures 3D and E**). Autofluorescence imaging in transparent mouse femur bone samples treated with 25% quadrol and 25% triethanolamine (TEA) showed no significant differences in autofluorescence signals for the two amino alcohols. However, mouse femur bones cleared with 25% triethanolamine (TEA) showed better resolution for deep imaging and increased transparency (**Figure 3F**).

We attempted to decrease the autofluorescence of bone by incubating the samples in two solutions in a prototype Bone-mPACT protocol, but it did not have much effect on the autofluorescence. Sudan Black (e.g., an autofluorescence quenching kit) was proposed for decreasing bone autofluorescence, but its use is limited in histological analysis to only thin bone slice16, and it does not allow for PACT-based bone clearing via Bone-mPACT. Nevertheless, identifying a replacement agent for quadrol was difficult, but triethanolamine (TEA) did increase the optical transparency during the bone clearing process.

연세대학교
YONSEI UNIVERSITY

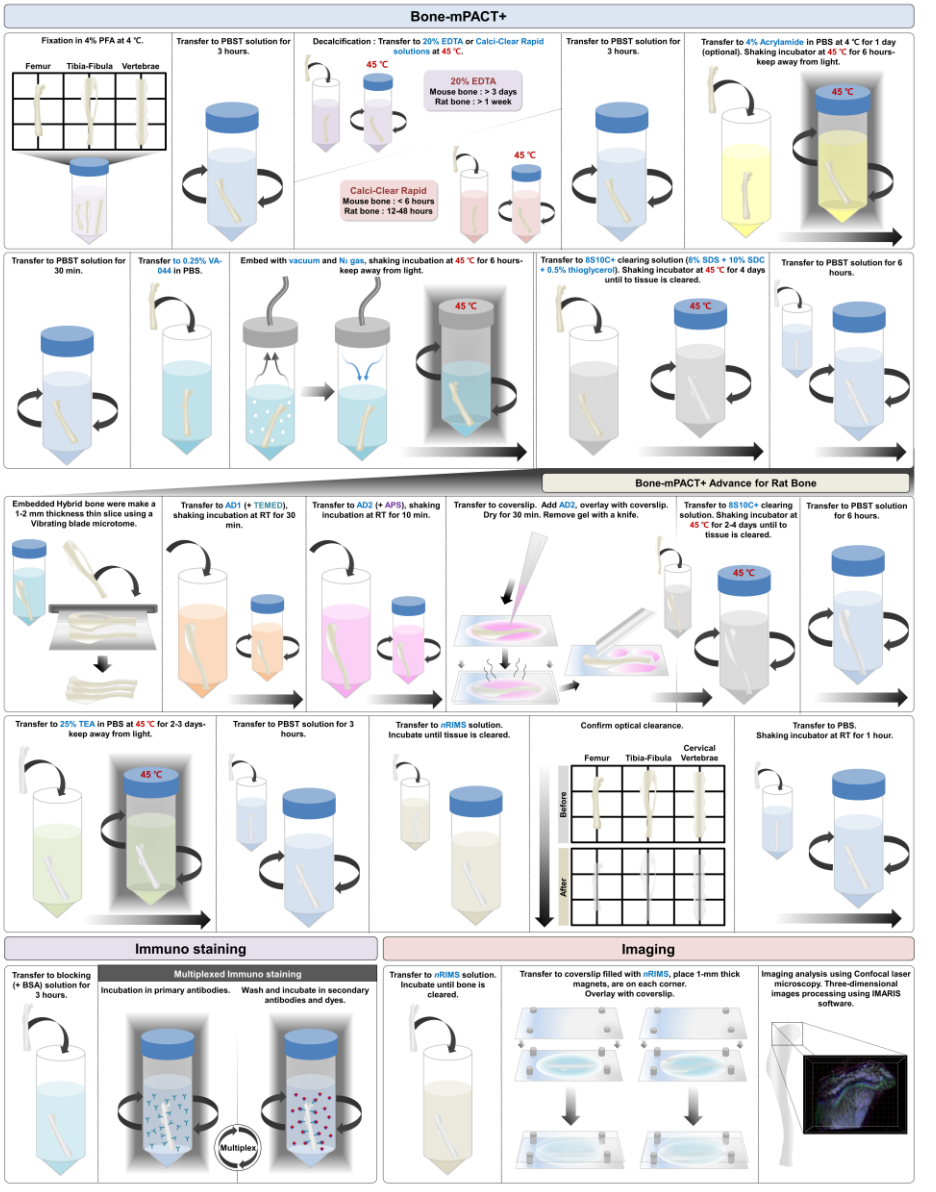

Figure 1. Schematic representation of Bone-mPACT+ optimized for rodent bones. The Bone-mPACT+ method involved the use of Calci-mPACT+ and 20EDTA-mPACT+ and was further optimized for processing rodent bones, which have a long clearing time during tissue processing. The Bone-mPACT+ Advance method was optimized for bone marrow and protected it from swelling.

연세대학교
YONSEI UNIVERSITY

Bone tissue sections with sizes larger than a mouse bone could be prepared in a 4% acrylamide-based hydrogel coating.

연세대학교
YONSEI UNIVERSITY

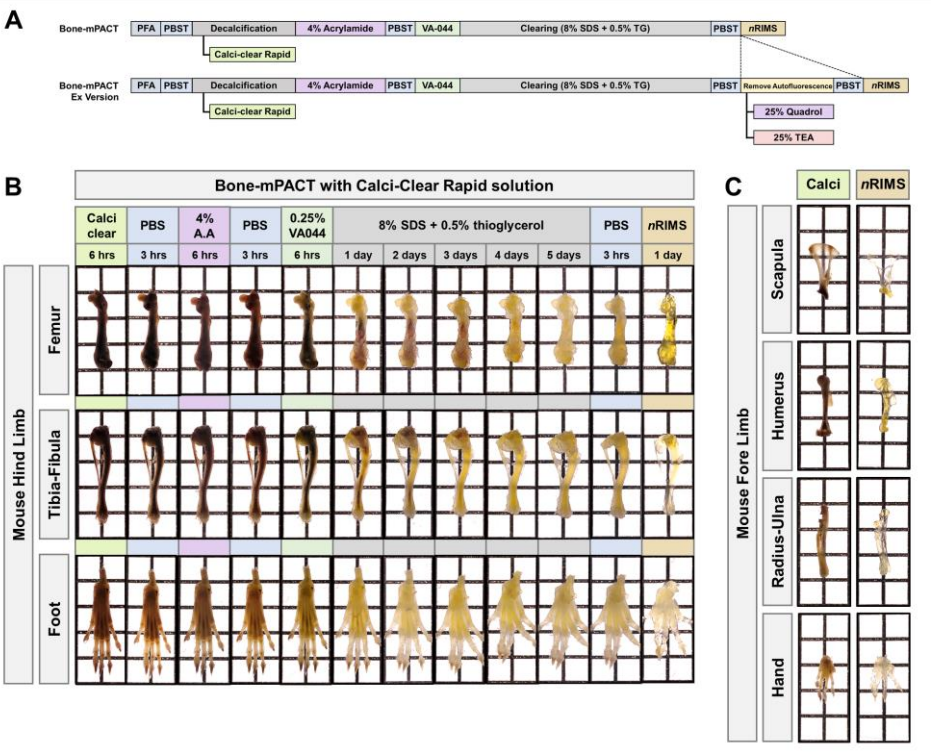

Figure 2. Generation of transparent mouse bones via Bone-mPACT for rapid clearing. (A) Schematic representation of passive tissue clearing methods. The individual reagents or processes used for decalcification and polymerization in the passive clearing methods are shown, including the additional incubation steps in Calci-Clear Rapid solution for rapid decalcification, and 25% *N,N,N',N'*-tetrakis(2-hydroxypropyl)ethylenediamine (quadrol) and 25% triethanolamine (TEA) solution to remove autofluorescence in the PACT-based modified prototype Bone-mPACT protocol. Comparison of optical transparency in the mouse hind limb bones (femur, tibia-fibula, and foot) (B) and mouse fore limb bones (scapula, humerus, radius-ulna, and hand) (C) achieved by Bone-mPACT with Calci-Clear Rapid solution. The transparency of all cleared samples was evident against a patterned background (length × width = 5 × 5 mm).

연세대학교
YONSEI UNIVERSITY

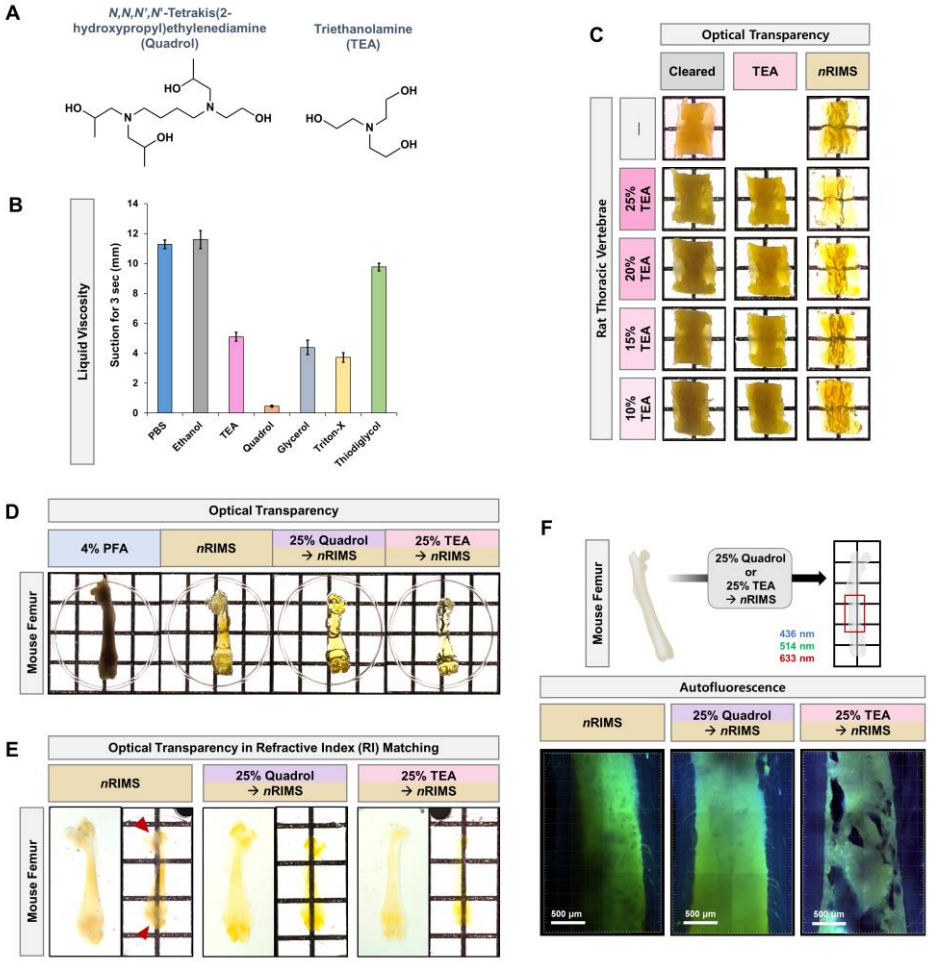

Figure 3. Optimization of Bone-mPACT for increasing the optical transparency. (A) Molecule of *N,N,N',N'*-tetrakis(2-hydroxypropyl) ethylenediamine (quadrol) and triethanolamine (TEA) reagents. (B) Comparison of liquid viscosity. (C) Comparison of optical transparency images in rat thoracic vertebrae achieved with 10–25% TEA incubation and refractive index matching. (D and E) Comparison of optical transparency images in mouse femurs achieved with 25% quadrol and 25% TEA incubation and refractive index matching with Bone-mPACT. The transparency of all cleared samples was evident against a patterned background (length × width = 5 × 5 mm). (F)

연세대학교
YONSEI UNIVERSITY

Comparison of autofluorescence images in mouse femur bone achieved with Bone-mPACT. Merged images with autofluorescence in green (514 nm), red (633 nm), and blue (436 nm). Scale bar (white: 500 μm).

연세대학교
YONSEI UNIVERSITY

2. Optimization of tissue clearing solution to preserve the tissue and provide rapid clearing.

PACT-based tissue clearing methods that use sodium dodecyl sulfate (SDS) can give rise to swelling effects in the clearing process of soft tissues, such as the brain, spinal cord, embryo, and other organs. As shown in **Figure 2B and C**, we confirmed tissue damage, in the form of shrinkage, in the hard bone samples cleared via the prototype Bone-mPACT protocol. This is an important issue in hard bone clearing via CLARITY-based tissue clearing protocols, and the presence of tissue damage confirmed the need for supplementation when decreasing the clearing time.

We prevented this problem in the present study by optimizing the tissue clearing solution. Takeyuki et al. showed that a potential clearing reagent, 10% sodium deoxycholate (SDC), increased the tissue clearing efficiency while maintaining biological structural stability during the clearing process[17]. We investigated the increased tissue clearing efficiency of sodium deoxycholate (SDC) by incorporating it into a PACT-based bone clearing method by preparing clearing solutions with the following combinations of sodium dodecyl sulfate (SDS), sodium deoxycholate (SDC), and α-thioglycerol (TG) (**Figure 4A**): 8S+: 8% SDS + 0.5% TG, 4S5C+: 4% SDS + 5% SDC + 0.5% TG, 8S5C: 8% SDS + 5% SDC + 0.5% TG, and 8S10C+: 8% SDS + 10% SDC + 0.5% TG.

As shown in **Figure 4B**, we compared the optical transparency in 1.5 mm thick mouse brain slices via five psPACTs and each clearing solution. Mouse brain slices were cleared in 8% SDS (8S) and 10% SDC (10C) at 45 °C for 2 days as controls, and the mouse brain slices cleared in 8% SDS showed similar swelling to that observed previously (after 4% PFA fixation). However, the mouse brain slices cleared in 10C for 2 days showed no change in size during the tissue clearing process. The 10C clearing solution showed an increasing optical tissue clearing efficiency, but confirming the optical transparency was

연세대학교
YONSEI UNIVERSITY

not easy because the image was more opaque than the image obtained with the 8S clearing solution.

We then compared the optical clearing transparency of mouse brain slices using the 8S+, 4S5C+, 8S5C+ and 8S10C+ clearly solutions using the psPACT protocol. The samples in the 8S5C+ and 8S10C+ treatments were rapidly cleared in 1 day, for a reduction in time expenditure of one full day, and the observed optical clearing patterns were of high-transparency grade. The brain slice cleared with 8S10C+ had a similar size to the original sample, whereas the brain slice cleared with 8S5C+ showed tissue swelling after clearing (**Figure 5A and B**).

We performed immunostaining for lectin to visualize blood vessels in intact mouse brains cleared via psPACT and in those cleared via the 10C, 8S5C+, and 8S10C+ solutions. Observation of the morphological structures of the mouse brain cleared with 10C or 8S10C+ at higher resolution (**Figure 5C**) revealed crystal formation in the 10C sample but no crystals in the 8S10C+ sample. The 8S10C+ cleared sample also did not undergo any color change during long-term storage at room temperature in a refractive index matching (*n*RIMS) solution (**Figure 5D**).

We also compared the optical tissue clearing efficiency of 8S10C+ in mouse embryos at the E13.5 and E17.5 embryonic stages. The mouse embryos cleared rapidly in 3–4 days (E13.5: 3 days, and E17.5: 4 days) in 8S10C+ without swelling or shrinkage, and the 8S10C+ samples showed higher optical transparency than the samples cleared in the 8S and 10C solutions (**Figure 6A-C**). These results indicate that the 8S10C+ combination of 8% SDS and 10% SDC was excellent for rapid tissue clearing and protected the tissue from the harsh clearing conditions.

연세대학교
YONSEI UNIVERSITY

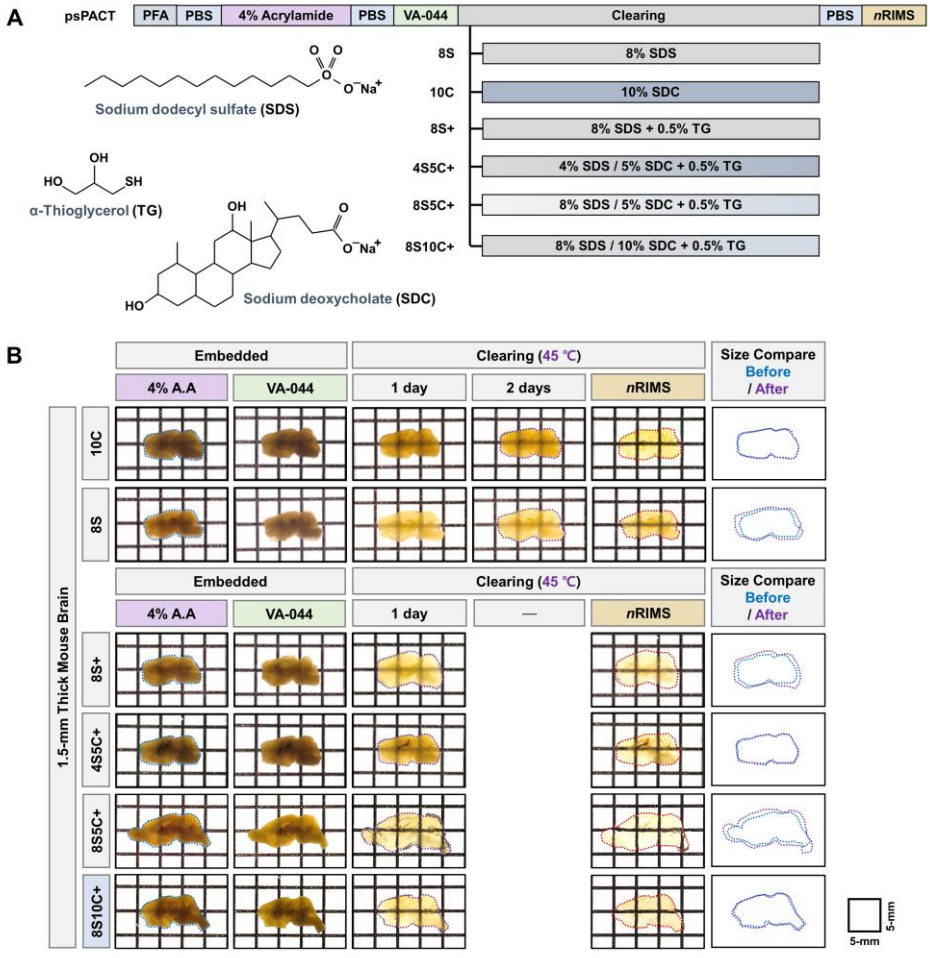

Figure 4. Generation of transparent mouse brain via modified psPACT. (A) Schematic representation of psPACT clearing methods. Clearing solutions were constructed by combining three reagents, sodium dodecyl sulfate (SDS), sodium deoxycholate (SDC), and α-thioglycerol (TG). The individual reagents or processes used for polymerization in the passive clearing methods are shown, including the various clearing solutions: 8S (8% SDS), 10S (10% SDS), 8S+ (8% SDS + 0.5% TG), 4S5C+ (4% SDS + 5% SDC + 0.5% TG), 8S5C+ (8% SDS + 5% SDC + 0.5% TG), and 8S10C+ (8% SDS + 10% SDC + 0.5% TG). (B) Comparison of optical transparency in the 1.5 mm thick mouse brain slices

연세대학교
YONSEI UNIVERSITY

using the psPACT protocol and six different clearing solutions. Right images indicate the sample size before and after clearing. Blue dotted line (4% AA), violet dotted line (after clearing), and red dotted line (after refractive index matching). The transparency of all the cleared samples was tested against a patterned background (length × width = 5 × 5 mm).

연세대학교
YONSEI UNIVERSITY

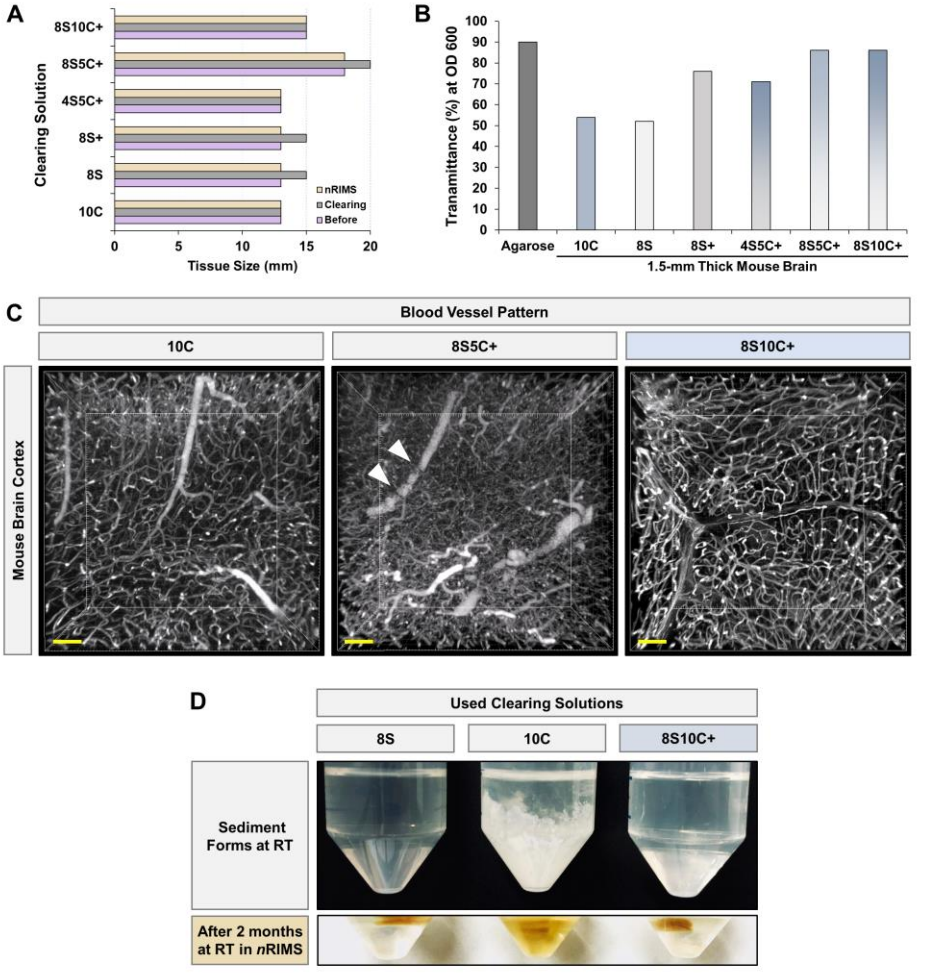

Figure 5. Comparison of blood vessel pattern of transparent mouse brain via modified psPACT. (A) Comparison of brain tissue size (see Figure 3B) during the clearing process. (B) Comparison of transmittance (%) of cleared brain samples at OD 600 nm. (C) Comparison of lectin immunohistochemical images of mouse brain cortex processed via psPACT with 10C, 8S5C+, and 8S10C+ clearing solutions. The lectin image for each sample was created from serial z-images (25 slices; depth: 500 μm) of the blood vessel pattern obtained by confocal microscopy at 10× magnification (0.45 NA, 2.0 mm working

연세대학교
YONSEI UNIVERSITY

distance), and the microscope was focused on a 1 × 1 panel (horizontal × vertical). Scale bar (white: 100 μm). (D) Comparison of clearing solutions (8S, 10C, and 8S10C+) and nRIMS in after tissue clearing.

연세대학교
YONSEI UNIVERSITY

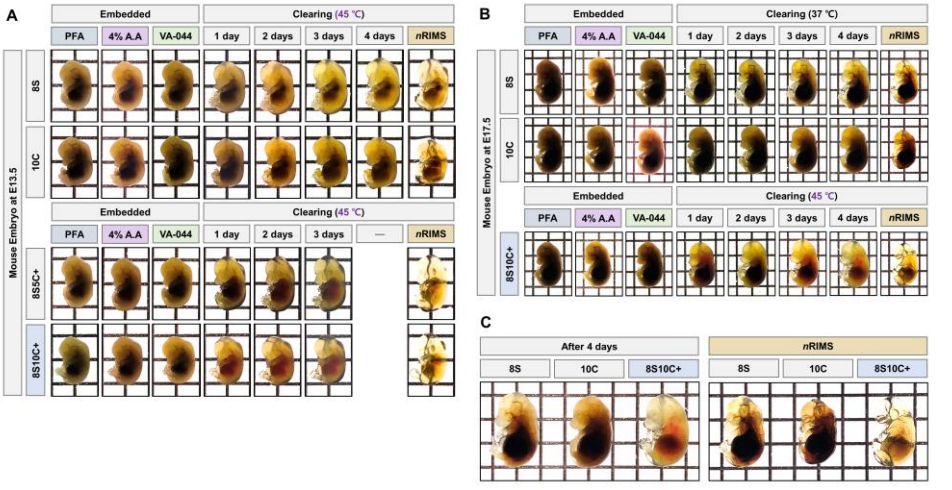

Figure 6. Generation of transparent mouse embryos via modified psPACT. Comparison of optical images in E13.5 (A) and E17.5 (B) mouse embryos using three or four clearing solutions in the IMPACT-Basic clearing process. (C) Comparison of the three clearing solutions in E17.5 mouse embryos after 4 days in 8S (left), 10C (middle), and 8S10C+ (right) clearing solutions. The transparency of all the cleared samples was tested against a patterned background (length × width = 5 × 5 mm).

연세대학교
YONSEI UNIVERSITY

3. Generation of transparent rodent bones via the Bone-mPACT+ method.

Our successful demonstration of the feasibility and efficiency of the 8S10C+ clearing solution and 25% triethanolamine (TEA) incubation was expanded to apply these optimizations to compare their efficacy with that of currently established bone clearing techniques. **Figure 1** shows the Bone-mPACT+ method, which included the use of two decalcification solutions (e.g., Calci-Clear and 20% EDTA). Two Bone-mPACT+ methods (Calci-mPACT+ and 20EDTA-mPACT+) were tested after each reagent. The Calci-mPACT+ and 20EDTA-mPACT+ protocols were based on the psPACT protocol of the polymerization process and combined with the 8S10C+ clearing step and the 25% triethanolamine (TEA) incubating step after clearing (**Figure 7A**).

The bone samples for the Calci-mPACT+ test were decalcified for 6 hours in Calci-Clear Rapid solution at 45 ℃ and then cleared for 4 days in 8S10C+ at 45 ℃, followed by post-incubation for 2 days in 25% triethanolamine (TEA) at 45 ℃. The end result was transparent bone in *n*RIMS solution. We generated a transparent mouse hind limb, including the femur, tibia-fibula, and foot, within 10 days using Calci-mPACT+ (**Figure 7B**). The Calci-mPACT+ cleared mouse bones showed no appearance changes or tissue damage, while displaying optimized clearing (compare to **Figure 2B**). The vertebrae in the Calci-mPACT+ samples were transparent after incubation for 3 days in the 8S10C+ clearing solution (**Figure 7C**).

The bone samples cleared with the 20EDTA-mPACT+ were decalcified for 3 days in 20% EDTA at 45 ℃ and then cleared for 4 days in 8S10C+ at 45 ℃, followed by post-incubation for 2 days in 25% triethanolamine (TEA) at 45 ℃. The end result was transparent bone, as determined by *n*RIMS solution. We generated the transparent mouse hind limb within 13 days via the 20EDTA-mPACT+ protocol (**Figure 8A**). Bones cleared in the 20EDTA-mPACT showed higher optical transparency than when cleared in Calci-mPACT+ and 10% SDC (10C) (**Figure 8B**), and the generated sample

연세대학교
YONSEI UNIVERSITY

size was better preserved than with 8S+ clearing after clearing (**Figure 8C**). Comparison of the autofluorescence imaging in the transparent mouse femur bone cleared with 20EDTA-mPACT+ and with Calci-mPACT+ after 25% quadrol and 25% triethanolamine (TEA) post-incubation revealed a similar significant decline in the autofluorescence of the heme-rich bone marrow (**Figure 8D**).

We also compared the previously reported bone clearing protocols (PEGASOS, CUBIC, and Bone-CLARITY) and 20EDTA-mPACT+ (**Figure 9**). The optical transparency of mouse tibia was higher after processing with 20EDTA-mPACT+ than with PEGASOS and CUBIC. Bone-CLARITY required 2 weeks for decalcification, and a longer passive clearing time of >5 days in 8% SDS.

Using these passive bone clearing methods, we were able to visualize intact, transparent models of the mouse bone, although the decalcification differed between the two methods. The optimized passive bone clearing methods achieved bone clarity in a short time. The results suggest that the Bone-mPACT+ bone clearing method that incorporates Calci-mPACT+ and 20EDTA-mPACT+ can generate clear bones more stably and rapidly than the previous passive clearing methods.

연세대학교
YONSEI UNIVERSITY

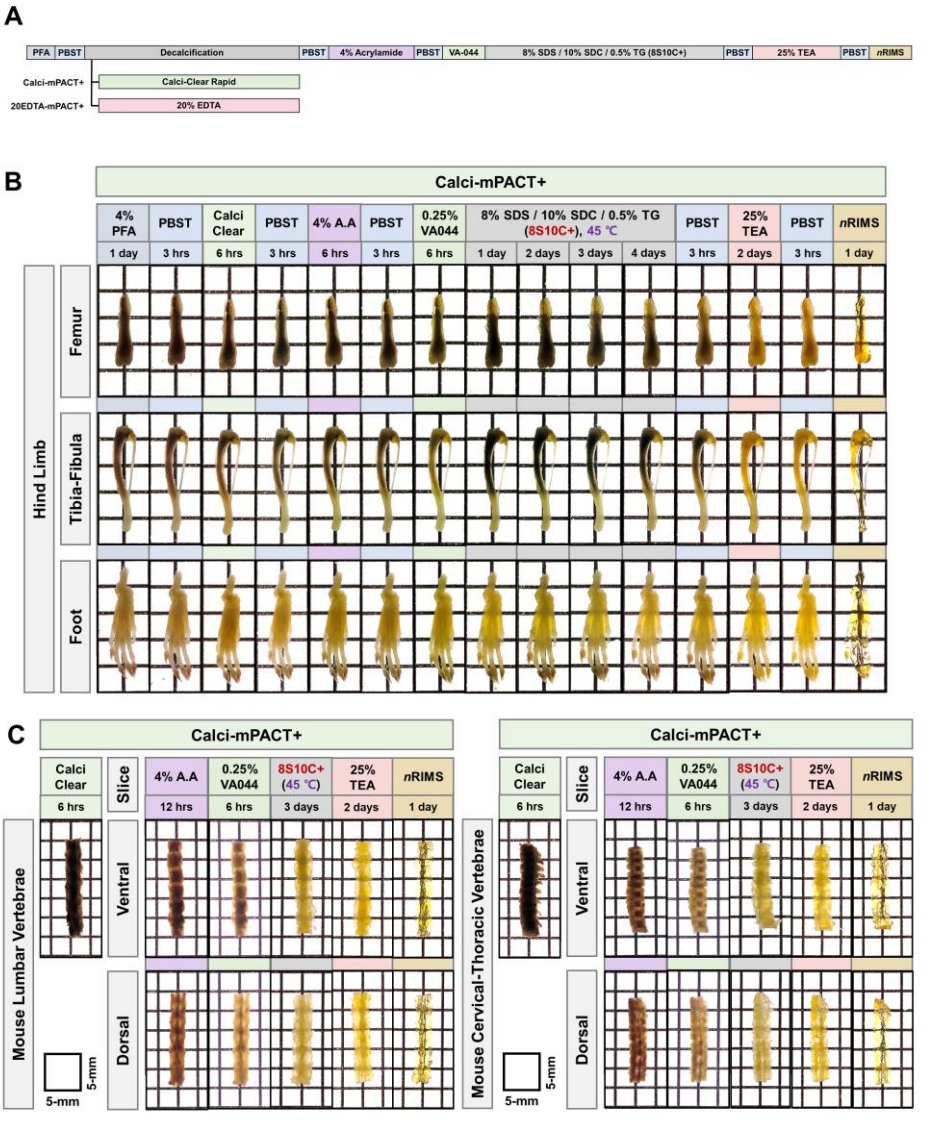

Figure 7. Generation of transparent mouse bones with Calci-mPACT+. Schematic representation of the optimized Bone-mPACT+ (Calci-mPACT+ and 20EDTA-mPACT+) method. Comparison of optical transparency in the mouse hind limb bones (femur, tibia-fibula, and foot) (B) and vertebrae (upper: lumbar, lower: cervical-thoracic) (C) achieved with the Calci-mPACT+ protocol. The

연세대학교
YONSEI UNIVERSITY

transparency of all cleared samples was tested against a patterned background (length × width=5 × 5 mm).

연세대학교
YONSEI UNIVERSITY

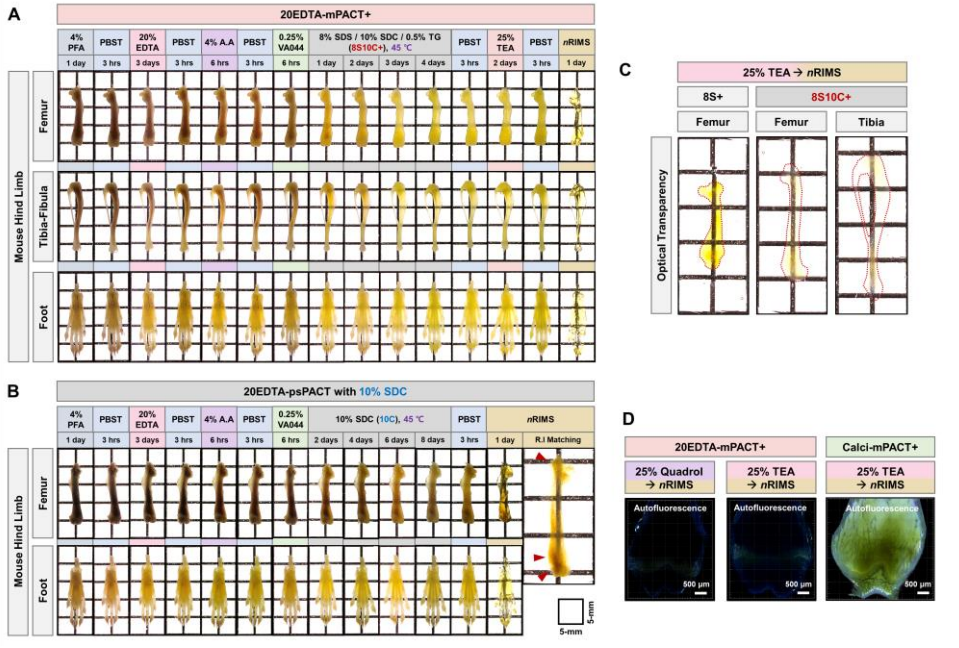

Figure 8. Generation of transparent mouse bones with 20EDTA-mPACT+. (A) Comparison of optical transparency in the mouse hind limb bones (femur, tibia-fibula, and foot) with the 20EDTA-mPACT+ protocol. (B) Comparison of the optical transparency in the mouse hind limb bones (femur and foot) achieved with the 20EDTA-psPACT protocol with 10% SDC (10C) clearing solution. (C) Presentation of the optical transparency with refractive index matching in mouse hind limb bones (femur and tibia) cleared using 8S+ (8% SDS+ 0.5% TG) and 8S 10C+ (8% SDS + 10% SDC + 0.5% TG) clearing solutions. The transparency of all cleared samples was tested against a patterned background (length × width=5 × 5 mm). (D) Comparison of autofluorescence images in adult mouse femurs after incubation with 25% quadrol and 25% TEA with the 20EDTA-mPACT+ and Calci-mPACT+ protocols. Merged images with autofluorescence in green (514 nm), red (633 nm), and blue (436 nm). Scale bar (white: 500 μm).

연세대학교
YONSEI UNIVERSITY

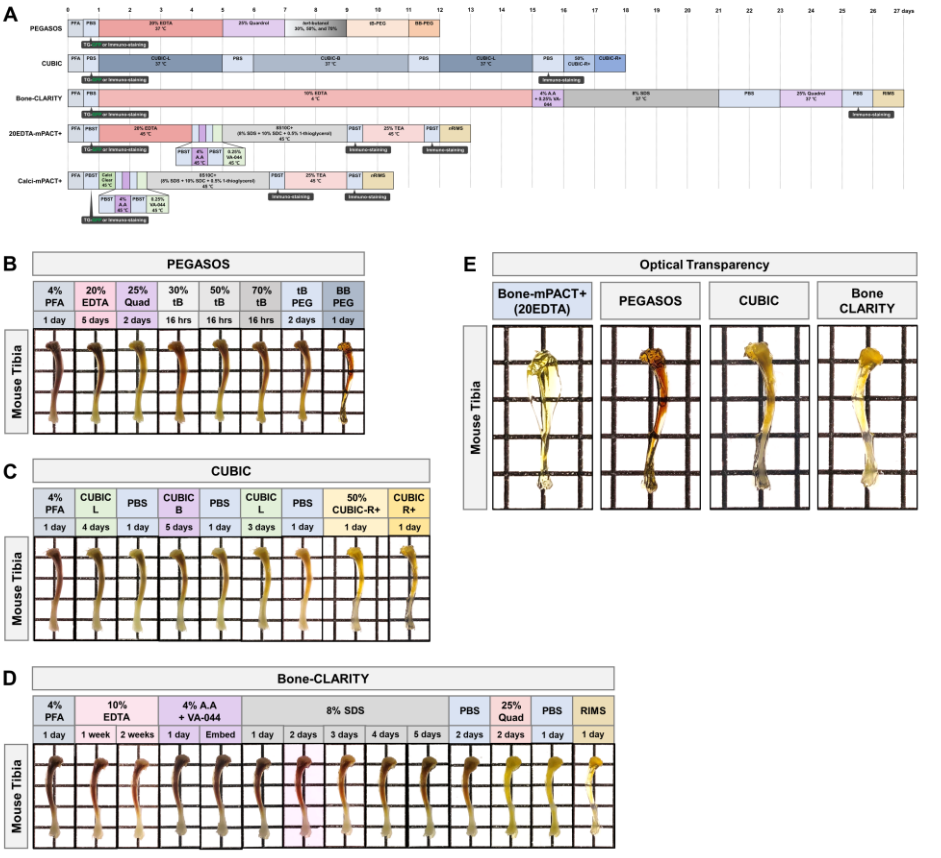

Figure 9. Generation of transparent mouse tibia by passive bone clearing methods. (A) Schematic representation and timeline of the passive bone clearing methods. The individual reagents or processes used for the decalcification and clearing process in the five clearing methods are shown. (B-E) Comparison of optical transparency achieved in mouse tibia processed via PEGASOS (B), CUBIC (C), Bone-CLARITY (D), and Bone-mPACT+ (20EDTA-mPACT+). The transparency of all the cleared samples was evident against a patterned background (length × width = 5 × 5 mm).

연세대학교
YONSEI UNIVERSITY

4. Investigation of bone metabolism in maternal mouse bone during pregnancy via Bone-mPACT+.

We applied Bone-mPACT+ to the vertebral column, a bone that is highly susceptible to fractures due to osteoporosis and whose complex geometry is particularly difficult to probe with traditional sectioning-based methods. We validated the Bone-mPACT+ protocol by applying our clearing and imaging method to investigate the marrow and trabecular patterns in the mother mouse femur and vertebrae bones from biopsies obtained during pregnancy. We isolated the femur and vertebrae bones from mother mice at 0, 13.5, and 17.5 days of gestation (typically 19–21 days in duration). The femur bone tissue was transparent in 10 days via Calci-mPACT+ with autofluorescence preservation (see **Figures 1 and 7**).

We visualized the endogenous fluorescence of the femur using Bone-mPACT+, and we compared the bone marrow and trabecular patterns of the focused condyle region in the mouse femur bone during pregnancy. We isolated the femur bone from mother mice at 0, 13.5, and 17.5 days during pregnancy. The femur bone tissue was transparent after 10 days with Calci-mPACT+ with autofluorescence preservation (see **Figure 7B**). We visualized the endogenous fluorescence of the femur using Bone-mPACT+, and we compared the bone marrow (highlighted region with autofluorescence) and trabecula (dark region) patterns focused condyle region in mouse femur bone during pregnancy. We saw a decrease in the bone size and an increase in the pore size of the bone marrow, and trabecular bone loss was significantly defined at 17.5 gestational days (**Figure 10A**). We cleared and imaged the vertebrae from these mice, focusing on the fourth lumbar vertebral body (L4), which is dense, opaque, and predominately composed of cancellous bone. Similar to the femur, the lumbar vertebra also showed trabecular bone loss at 17.5 gestational days (**Figure 10B**).

We then performed immunostaining for Runt-related transcription factor-2

연세대학교
YONSEI UNIVERSITY

(RUNX2) and osteoprotegerin (OPG) in the maternal tibia bone at 17.5 gestational days after processing with Calci-mPACT+. Endogenous fluorescence complicated the immunohistochemistry, but at 17.5 gestational days, RUNX2 and osteoprotegerin (OPG) expression was still concentrated in the trabecular and plane regions of the proximal end and showed autofluorescence of the bone marrow (**Figure 10C**). Immunostaining for lectin and osteoprotegerin (OPG) in maternal femur bones processed by 20EDTA-mPACT+ at 17.5 gestational days revealed that osteoprotegerin (OPG) expression was still concentrated in the bone marrow regions containing osteoblasts (e.g., the distal head and diaphysis), and in the bloodstream (**Figure 11A**). In the tibias at 17.5 gestational days, osteoprotegerin (OPG) was also expressed in the bone marrow containing osteoblasts (e.g., the trabecular and proximal end of the plane regions), but the bone marrow showed little autofluorescence (**Figure 11B**). These changes in bone density suggest that pregnancy is associated with a deterioration of the maternal bone mass. The metabolism of calcium resets to cover the needs imposed by the building of the fetal skeleton[18,19]. During pregnancy and lactation, the mother has an increased need for calcium to meet the fetal calcium requirements[20,21].

연세대학교
YONSEI UNIVERSITY

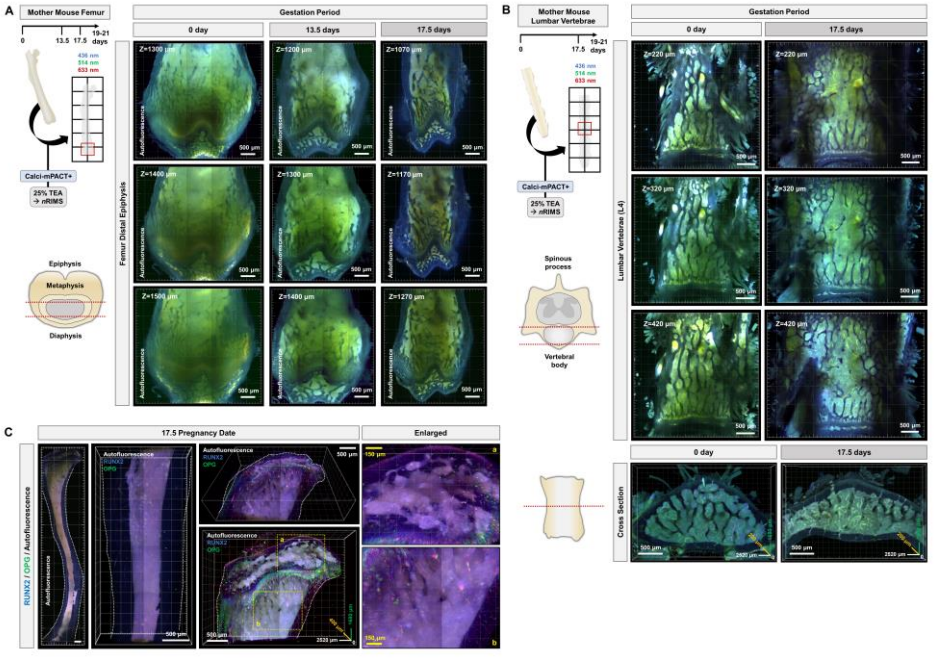

Figure 10. Autofluorescence detection and OPG expression in female mouse bones during pregnancy. (A and B) Comparison of endogenous fluorescence images in transparent maternal mouse femur bones (A) and fourth lumbar vertebrae (B) via Calci-mPACT+. Single z-stack images of bones at (left) 0 date, (middle) 13.5 gestational days, and (right), and 17.5 gestational days (gestation = 21 days). Merged images with autofluorescence in green (514 nm), red (633 nm), and blue (436 nm). Scale bar (white: 500-μm). (C) RUNX2 (green) and OPG (blue) expression images acquired with a 10× objective on a confocal laser microscope in maternal mouse tibia bone at 17.5 gestational days obtained with Calci-mPACT+. (Left) Whole endogenous fluorescence images of the tibia (3 × 20 tiled, z=390 μm), (middle and right) 3D projection of the RUNX2 and OPG expression focusing on the middle region (4 × 8 tiled, range: 300 μm), and proximal end (5 × 6 tiled, range: 800 μm), including the plane regions in the tibia. Autofluorescence is preserved in the bone marrow. Scale bar (white: 500 μm).

연세대학교
YONSEI UNIVERSITY

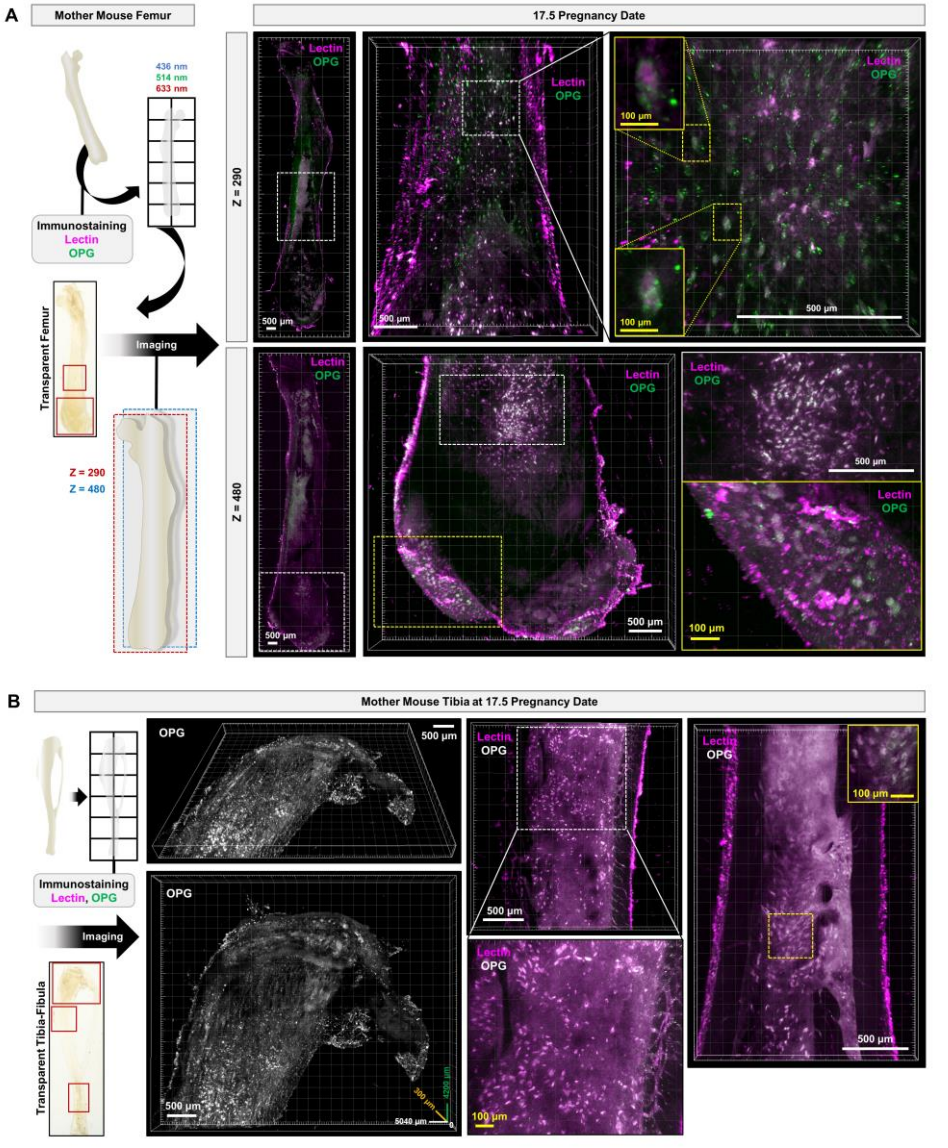

Figure 11. OPG expression in female mouse bones during pregnancy. (A and B) Immunohistochemistry images of OPG expression in the bone marrow in the cleared femur and tibia of maternal mouse tibia bone at 17.5 gestational days using 20EDTA-mPACT+. OPG and lectin immunostaining in adult female mouse femur and tibia processed with 20EDTA-mPACT+. (A) 3D projection of

연세대학교
YONSEI UNIVERSITY

OPG (green) expression, focusing on the distal head (4 × 4 tiled, range: 400 μm) and diaphysis (3 × 4 tiled, range: 250 μm) in the femur, including the bone marrow; (left) the upper (z=290 μm) and lower (z=480 μm) images were 4 × 16 tiled. (B) 3D projection of OPG (white) expression focusing on the trabecular (5 × 6 tiled, range: 300 μm) and plane regions at the proximal end (3 × 3 and 3 × 4 tiled, range: 100 μm) of the tibia, including the bone marrow. Scale bar (white: 500 μm, yellow: 100 μm).

연세대학교
YONSEI UNIVERSITY

5. Investigation of bone metabolism via Bone-mPACT+ in a male osteoporosis rat model.

We next applied Calci-mPACT+ to the rat vertebral column of a male osteoporosis model generated by orchiectomy[22]. The vertebrae are highly susceptible to fractures due to osteoporosis, and their complex geometry is particularly difficult to probe with traditional sectioning-based methods. We cleared and imaged the vertebrae from the rat models, focusing on the second lumbar vertebral body (L2). As shown in **Figure 12A and B**, the rat vertebral column was cleared after 6 days of Calci-mPACT+ treatment, and optical deep imaging of the vertebrae was possible after treatment with 25% TEA, which left the bones even more diaphanous. We also visualized the endogenous fluorescence in vertebrae from sham rats and at 8 weeks after orchiectomy, and we compared the bone marrow (highlighted region with autofluorescence) and trabecular (dark region) patterns. We confirmed a decrease in bone size and an increase in the bone marrow pore size; trabecular bone loss was especially defined after orchiectomized 8 weeks (**Figure 12C**). These results provided a proof-of-concept demonstration that our Bone-mPACT+ method can be used to perform three-dimensional analyses of biological structures in whole intact rodent bones.

To demonstrate proof-of-concept, we processed 1 mm-thick femur bone slices derived from the male rat model of osteoporosis according to our Bone-mPACT+ Advance protocols. Briefly, we generated male osteoporosis model (after 8 weeks) with orchiectomy, respectively, and analyzed mice for bone densitometry (**Figure 8B**).

연세대학교
YONSEI UNIVERSITY

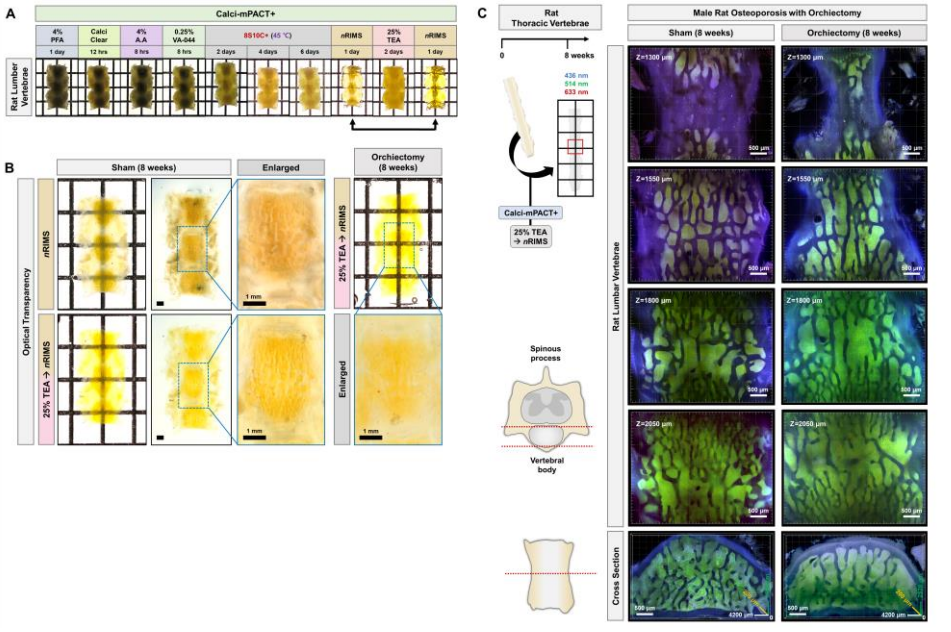

Figure 12. Endogenous fluorescence detection in transparent vertebrae of male osteoporosis model rats. (A) Comparison of optical transparency achieved in rat lumbar vertebrae using Calci-mPACT+. (B) Comparison of optical transparency achieved in the rat lumbar vertebral column (L2) of sham-operated rats and orchiectomized rats 8 weeks after the operation. Samples were processed with Calci-mPACT+. The transparency of all the cleared samples was tested against a patterned background (length × width = 5 × 5 mm). Scale bar (black: 1-mm). (C) Comparison of endogenous fluorescence images in the transparent rat lumbar vertebral column (L2) of sham-operated and orchiectomized rats 8 weeks after the operation. Merged images showing autofluorescence in green (514 nm), red (633 nm), and blue (436 nm). Scale bar (white: 500 μm).

연세대학교
YONSEI UNIVERSITY

6. Development of a bone-specific Bone-mPACT+ Advance protocol for bone tissue clarity and retention of intact structure in large bone sections.

The Bone-mPACT+ protocol (20EDTA-mPACT+ and Calci-mPACT+) successfully allowed imaging of mouse bone; however, we found that large bones and bones from larger rodents were difficult to assess due to the limited 2 mm working distance of the objective lens in a conventional confocal laser microscope. Large samples can be visualized using light-sheet fluorescent microscopy (LSFM); however, the technique is not amenable to most traditional laboratories due to limited equipment availability and high associated costs23. Wide applicability of the Bone-mPACT+ protocol is further limited by the long time required for tissue processing (e.g., clearing alone requires a minimum of >10 days, followed by an additional >10 days for immunostaining).

To address this issue, we optimized our Bone-mPACT+ method specifically for processing sections of rat bones; we named this new protocol Bone-mPACT+ Advance. The Bone-mPACT+ also used an ammonium persulfate (APS) and tetramethyl ethylenediamine (TEMED)-based solution for embedding, as opposed to the VA-044 azo initiator used in the original CLARITY protocol1. As shown in Figure 1, Bone-mPACT+ Advance follows the same steps as the two-step Bone-mPACT+ (20EDTA-mPACT+ and Calci-mPACT+) protocol, but after the second incubation in IM1, the rat bones are sliced into thin sections at a thickness of roughly a third of the original embryo and incubated in a 4% acrylamide-based solution containing TEMED (AD1) and then a 4% acrylamide-based solution containing APS (AD2) prior to clearing24. The Bone-mPACT+ Advance method successfully achieved optical clearance of rat tibia bone sections within 2 weeks (decalcification times with 20% EDTA: 1 week, and clearing times with 8S10C+: 4 days), with little tissue damage (**Figure 13A**). We provided a proof-of-concept demonstration by processing 2-mm thick femur and tibia bone slices derived from the male rat osteoporosis model according to our “Bone-mPACT+ Advance” protocols with

연세대학교
YONSEI UNIVERSITY

Calci-Clear Rapid solution. We visualized the endogenous fluorescence in femur and tibia bones of male orchiectomy rat model at after 8 weeks, and we observed the bone marrow (highlighted region with autofluorescence) and trabecular (dark region) patterns with high-resolution imaging (**Figure 13B and C**).

연세대학교
YONSEI UNIVERSITY

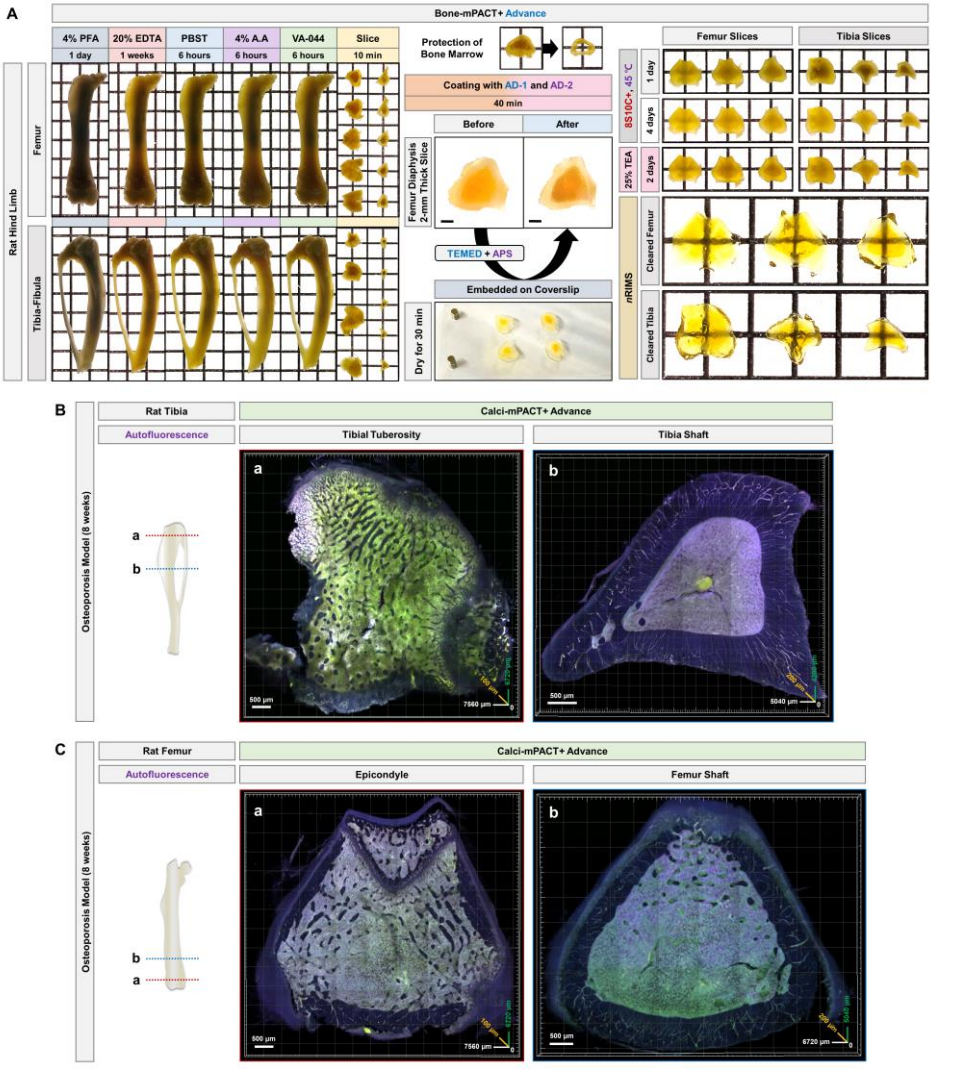

Figure 13. Bone-mPACT+ Advance for large bone. (A) Comparison of optical transparency achieved in rat femur and tibia bones using Bone-mPACT+ Advance with 20% EDTA. The transparency of all cleared samples was evident against a patterned background (length:width=5 mm:5 mm). (B and C) High-resolution autofluorescence images of rat tibia and femur bones of orchiectomized rats 8 weeks after the operation using Bone-mPACT+ Advance with Calci-Clear Rapid solution. (B) Endogenous fluorescence images of the

연세대학교
YONSEI UNIVERSITY

tibial tuberosity (a; 9 × 8 tiled, range: 100 μm) and shaft (b; 6 × 5 tiled, depth: 200 μm) in the transparent rat tibia of orchiectomized rats 8 weeks after the operation. (C) Endogenous fluorescence images of the epicondyle (a; 9 × 8 tiled, range: 100 μm) and shaft (b; 8 × 6 tiled, range: 200 μm) in the transparent rat femur of orchiectomized rats 8 weeks after the operation. Merged images with autofluorescence in green (wave length: 514 nm), red (wave length: 633 nm), and blue (wave length: 436 nm). Scale bar (white: 500 μm).

연세대학교
YONSEI UNIVERSITY

7. Investigation of RANKL and PRDM family expression pattern in male rat bones.

We also provided a proof-of-concept demonstration by processing femur and tibia bone slices derived from the male rat osteoporosis model according to our "Bone-mPACT+ Advance" protocols with 20% EDTA. We then performed immunostaining for RANKL and PRDM family members (PRDM10 and PRDM12) in femur and tibia bone slices of osteoporosis male rat models processed by Bone-mPACT+ Advance with 20% EDTA. RANKL expression was still concentrated in the bone surface and in the bone marrow and proximal region, whereas PRDM10 was expressed in the developing skeletal cartilage in the embryonic developmental stage[24,25], and we hypothesized that it plays an important role in bone formation and degenerative diseases, such as osteoporosis. PRDM10 and PRDM12 were also expressed in the bone marrow in the proximal tibia (**Figure 14A and B**).

We also visualized the PRDM10 and PRDM12 expression of the femur and tibia using 20EDTA-mPACT+, and we compared the PRDM10 and PRDM12 expression patterns in mouse femur bone during pregnancy. Similar to male rat osteoporosis model, PRDM10 was also expressed similar to RANKL in the bone surface and bone marrow in the proximal region in the female mouse bones. Whereas specific expression (number of cells) of PRDM10 and PRDM12 were decreased in comparison with 0 day in the mouse bones at 17.5 gestational days[26] (**Figure 15A and B**). The especially high levels of PRDM10 and PRDM12 expression in regions that also expressed OPG/RANKL suggest that the PRDM proteins may have critical functions in the development of the regressive changes seen in osteoporotic bone.

연세대학교
YONSEI UNIVERSITY

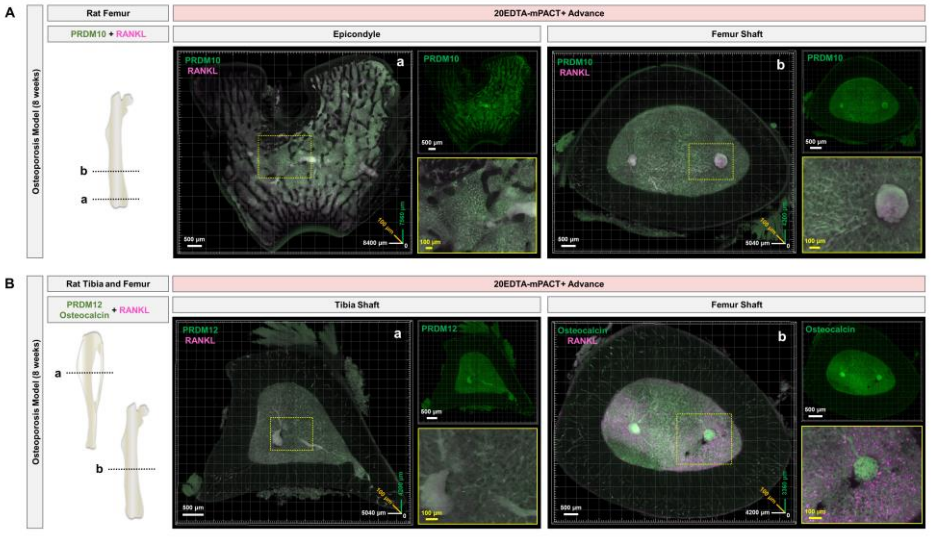

Figure 14. PRDM10 and PRDM12 expression in male osteoporosis model rats. (A and B) High-resolution autofluorescence images of rat tibia and femur bones of orchiectomized rats 8 weeks after the operation using Bone-mPACT+ Advance with 20% EDTA. (A) PRDM10 and RANKL immunostaining in femur (left: epicondyle (10 × 9 tiled), and right: shaft (6 × 5 tiled)) and tibia bones 8 weeks after the orchiectomy operation. (B) PRDM12, RANKL and osteocalcin immunostaining in tibia (6 × 5 tiled) and femur (5 × 4 tiled) bones 8 weeks after the orchiectomy operation. All section images were tile scanned and z-stacked (range: 100 μm). All section images were tile scanned (femur: 4 × 6 tiled, and tibia: 5 × 4 tiled) and z-stacked (range: 200 μm). Scale bar (white: 500 μm, yellow: 100 μm).

연세대학교
YONSEI UNIVERSITY

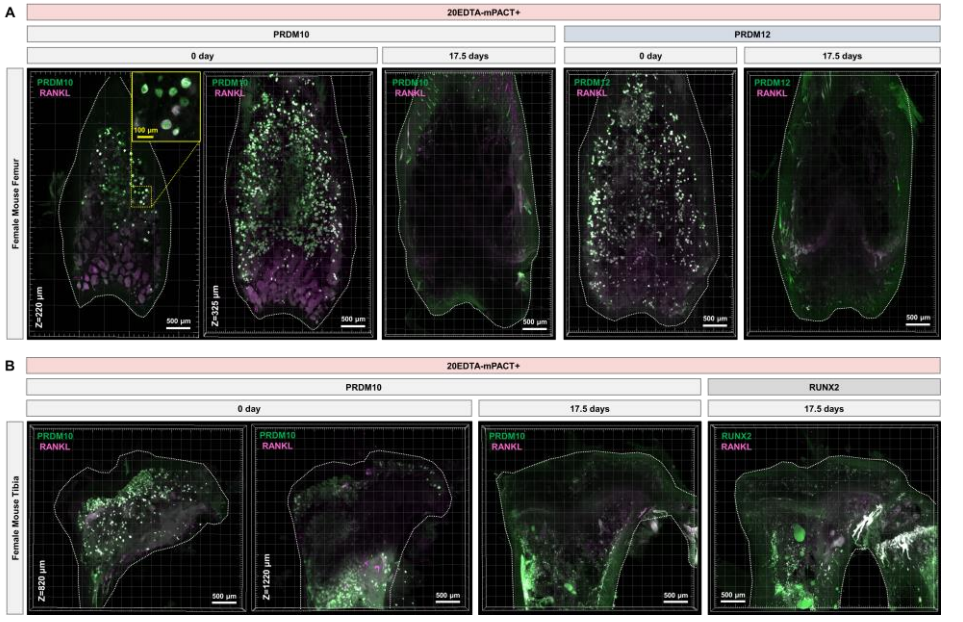

Figure 15. PRDM10 and PRDM12 expression in female mouse bones during pregnancy. (A) PRDM10, PRDM12 and RANKL immunostaining in femur bones at 0 date and 17.5 gestational days. (B) PRDM10, RANKL and RUNX2 immunostaining in tibia bones at 0 date and 17.5 gestational days. All section images were tile scanned (femur: 4 × 6 tiled, and tibia: 5 × 4 tiled) and z-stacked (range: 200 μm). Scale bar (white: 500 μm, yellow: 100 μm).

연세대학교
YONSEI UNIVERSITY

IV. DISCUSSION

We previously described a process-separate passive clearing technique (psPACT) and a modified PACT (mPACT) that allow the rapid achievement of optical transparency with limited equipment and minimal hands-on processing time and without a requirement for electrophoretic tissueclearing[3-5]. When applied to whole mouse CNS tissue and embryos, psPACT and mPACT significantly improved tissue transparency compared to existing methods[5,24]. Here, we present an optimized PACT-based protocol for hard bone clearing, Bone-mPACT+, which was specifically optimized to achieve optical transparency in intact rodent bones, again without the need for electrophoretic tissue clearing.

While the original CLARITY method significantly advanced our understanding of the three-dimensional relationships between biological structures with unprecedented detail, its relatively harsh treatments are not amenable to clearing rodent bones[1]. For this reason, various methodologies have been developed specifically for mouse bone tissue, but they are not without their own limitations. For instance, Bone-CLARITY (an optimized version of PACT-deCAL) requires roughly four weeks to achieve optical transparency with its decalcification process at low temperature (i.e., 4 °C) in 10% EDTA[6,15]. By contrast, 3DISCO[26], CUBIC[27-29] and PEGASOS[7] rapidly generate transparent bones within 2 weeks, but their use of organic solvents can interfere with immunostaining and produce undesired artifacts[30].

The CLARITY-based PACT tissue clearing protocol involves the use of a hybrid tissue hydrogel embedded with 4% acrylamide and photoinitiator (0.25% VA-044), and the transparent tissue is finally generated with an extra incubation in 8% sodium dodecyl sulfate (SDS) clearing solution after embedding. The hybrid PACT sample shows obvious tissue swelling during the clearing step. In these clearing processes, tissue damage and expansion during clearing of the

연세대학교
YONSEI UNIVERSITY

hard bone tissue clearing are major problems and create structural differences between the hard tissues and the internal bone marrow.

Hard bone tissue requires a decalcification step to remove minerals and prevent changes to soft tissue before bone clearing, and intact bone is easily decalcified by incubation in 10–20% EDTA, as previously reported[6,7,31-33]. Decalcification in EDTA was accelerated at >37 °C, but EDTA at room temperature or low temperature (4 °C) provided optimal results for immunohistochemistry and cellular and structural details. However, this decalcification requires a long time32. The Bone-mPACT+ protocol decreases the decalcification time with incubation at 45 °C in 20% EDTA and the use of Calci-Clear Rapid solutions.

Sodium deoxycholate (SDC) has not been deemed applicable for use in animal tissues[2,29]; however, SDC clearing has resulted in the best optical transparency, and it rendered the mouse brain fully transparent after RI matching with ScaleCUBIC-2[17]. In the present study, to ensure retention of bone structural integrity and to prevent hydrogel expansion with rapid tissue clearing, we optimized the tissue clearing process of psPACT with a clearing solution (8S10C+) by mixing 8% SDS and 10% SDC with 0.5% α-thioglycerol (TG). As shown in **Figure 4**, mouse brain slices and embryos processed by psPACT with 8S10C+ clearing solution showed rapid clearing efficiency and high optical transparency. The combination of 8S10C+ and SDC showed the best clearing efficiency, at least under our psPACT conditions. The average light-transmittance ratio was slightly higher for the 8S10C+ cleared tissues than for the SDS-cleared and SDC-cleared tissues.

We also removed the autofluorescence of bone cleared using Bone-mPACT+ by incorporating an additional incubation step with 25% TEA, which is more readily available and less expensive than amino alcohols like quadrol[6,7]. As shown in **Figure 7 and 8**, mouse bone tissues processed through Bone-mPACT+, involving Calci-mPACT+ (total: 10 days) and

연세대학교
YONSEI UNIVERSITY

20EDTA-mPACT+ (total: 13 days), showed greater resistance to tissue swelling after clearing. Bone-mPACT+ provides high optical transparency of both soft and hard tissues with rapid clearing in 8S10C+ clearing solution and post-incubation in 25% TEA at 45 °C. Therefore, we further optimized Bone-mPACT+ for clearing thin sections as opposed to large rat bone tissues. This protocol, which we termed Bone-mPACT+ Advance, involves processing rat bone via Bone-mPACT+ up to the hydrogelation step, followed by thin slicing and subsequent incubation in AD1 and AD2. Slices of rat bone were successfully cleared via Bone-mPACT+ Advance with minimal damage to tissue integrity.

For a proof-of-concept demonstration, we investigated the bone marrow and trabecular pattern of maternal femur and lumbar vertebrae bones cleared via the Calci-mPACT+ method during mouse pregnancy. At 13.5 and 17.5 gestational days (full gestation = 19–21 days), the bone size had decreased and the bone marrow pore size had increased; the trabecular bone loss was especially defined. These results are similar to the observations made in the lumbar vertebrae of male osteoporosis model rats following orchiectomy[22,34]. We investigated the expression of osteoprotegerin (OPG) and visualized the blood vessels with lectin staining in the mouse femur and tibia bones made transparent with 20EDTA-mPACT+.

We also observed PRDM10 and PRDM12 expression with receptor activator of NF κB ligand (RANKL) expression in transparent femur and tibia bones from male osteoporosis model rats and female mouse during pregnancy using Bone-mPACT+ and Bone-mPACT+ Advance. PRDM10 and PRDM12 have been implicated in both vertebrate development and cancer, but their expression profiles and function are less well characterized relative to other members of the PRDM family[35,36]. Consistent with previous reports of PRDM10 and its role in the development of sensory neurons and cartilage[24,25], we showed that PRDM10 is expressed in bone marrow in the proximal tibias of male osteoporosis model

연세대학교
YONSEI UNIVERSITY

rats. PRDM12 was also primarily expressed in bone marrow in the proximal tibia. PRDM10 and PRDM12 were also expressed in the bone marrow in the femur and tibia in female mouse. In contrast, for the first time, we found for the first time that the marrow adipocyte or putative mesenchymal stromal cells (MSC) containing PRDM10 and PRDM12 expression were decreased in the femur and tibia in female mouse during pregnancy.

Our results established, for the first time, the expression profiles of PRDM10 and PRDM12 with RANKL/OPG in intact rodent osteoporotic bones using a tissue clearing technique. Importantly, these studies have demonstrated the feasibility and efficacy of using Bone-mPACT+ and advanced type (Bone-mPACT+ Advance) for clearing bones derived from experimental animals, thereby further broadening the applicability of CLARITY-based methods for studying biological structures[6]. In addition, our results identify a powerful investigative tool for structural characterization of bones using 3D analysis of intact bone in experimental animals. Bone-mPACT+ facilitates the rapid examination of 3D morphological and therapeutic aspects of surgical animal disease models and can be used to aid in the investigation of medical conditions, such as serious degenerative disease, bone cancers, and malformations, and for surgical studies.

연세대학교
YONSEI UNIVERSITY

V. CONCLUSION

Our Bone-mPACT+ protocol significantly improves the optical transparency of hard bone tissues, it is faster than traditional passive clearing methods, and it requires limited equipment and minimal hands-on processing time. Our data suggest that our Bone-mPACT+ and Bone-mPACT+ Advance protocols could provide access to stereoscopic multiscale information that will expand the current understanding of health and disease.

연세대학교
YONSEI UNIVERSITY

REFERENCES

1. Chung K, Wallace J, Kim SY, Kalyanasundaram S, Andalman AS, Davidson TJ, et al. Structural and molecular interrogation of intact biological systems. Nature 2013;497:332-7.
2. Yang B, Treweek JB, Kulkarni RP, Deverman BE, Chen CK, Lubeck E, et al. Single-cell phenotyping within transparent intact tissue through whole-body clearing. Cell 2014;158:945-58.
3. Woo J, Lee M, Seo JM, Park HS, Cho YE. Optimization of the optical transparency of rodent tissues by modified PACT-based passive clearing. Exp Mol Med 2016;48:e274.
4. Woo J, Lee EY, Park HS, Park JY, Cho YE. Novel Passive Clearing Methods for the Rapid Production of Optical Transparency in Whole CNS Tissue. J Vis Exp 2018.
5. Woo J, Kang H, Lee EY, Park S, Cho YE. Investigation of PRDM7 and PRDM12 expression pattern during mouse embryonic development by using a modified passive clearing technique. Biochem Biophys Res Commun 2020;524:346-53.
6. Greenbaum A, Chan KY, Dobreva T, Brown D, Balani DH, Boyce R, et al. Bone CLARITY: Clearing, imaging, and computational analysis of osteoprogenitors within intact bone marrow. Sci Transl Med 2017;9.
7. Jing D, Zhang S, Luo W, Gao X, Men Y, Ma C, et al. Tissue clearing of both hard and soft tissue organs with the PEGASOS method. Cell Res 2018;28:803-18.
8. Jones DH, Kong YY, Penninger JM. Role of RANKL and RANK in bone loss and arthritis. Ann Rheum Dis 2002;61 Suppl 2:ii32-9.
9. Du T, Yan Z, Zhu S, Chen G, Wang L, Ye Z, et al. QKI deficiency leads to osteoporosis by promoting RANKL-induced osteoclastogenesis and

연세대학교
YONSEI UNIVERSITY

disrupting bone metabolism. Cell Death Dis 2020;11:330.

10. Min H, Morony S, Sarosi I, Dunstan CR, Capparelli C, Scully S, et al. Osteoprotegerin reverses osteoporosis by inhibiting endosteal osteoclasts and prevents vascular calcification by blocking a process resembling osteoclastogenesis. J Exp Med 2000;192:463-74.
11. Chen N, Hu T, Gui Y, Gao J, Li Z, Huang S. Transcriptional regulation of Bcl-2 gene by the PR/SET domain family member PRDM10. PeerJ 2019;7:e6941.
12. Han BY, Seah MKY, Brooks IR, Quek DHP, Huxley DR, Foo CS, et al. Global translation during early development depends on the essential transcription factor PRDM10. Nat Commun 2020;11:3603.
13. Vermeiren S, Bellefroid EJ, Desiderio S. Vertebrate Sensory Ganglia: Common and Divergent Features of the Transcriptional Programs Generating Their Functional Specialization. Front Cell Dev Biol 2020;8:587699.
14. Bartesaghi L, Wang Y, Fontanet P, Wanderoy S, Berger F, Wu H, et al. PRDM12 Is Required for Initiation of the Nociceptive Neuron Lineage during Neurogenesis. Cell Rep 2019;26:3484-92 e4.
15. Treweek JB, Chan KY, Flytzanis NC, Yang B, Deverman BE, Greenbaum A, et al. Whole-body tissue stabilization and selective extractions via tissue-hydrogel hybrids for high-resolution intact circuit mapping and phenotyping. Nat Protoc 2015;10:1860-96.
16. Schnell SA, Staines WA, Wessendorf MW. Reduction of lipofuscin-like autofluorescence in fluorescently labeled tissue. J Histochem Cytochem 1999;47:719-30.
17. Miyawaki T, Morikawa S, Susaki EA, Nakashima A, Takeuchi H, Yamaguchi S, et al. Visualization and molecular characterization of whole-brain vascular networks with capillary resolution. Nat Commun 2020;11:1104.
18. Sanz-Salvador L, Garcia-Perez MA, Tarin JJ, Cano A. Bone metabolic

연세대학교
YONSEI UNIVERSITY

changes during pregnancy: a period of vulnerability to osteoporosis and fracture. Eur J Endocrinol 2015;172:R53-65.

19. Jia H, Rao L, Miu KK, Tang S, Chen W, Yang G, et al. Inhibited Maternal Bone Resorption Suppress Fetal Rat Bone Development During Pregnancy. Front Cell Dev Biol 2020;8:83.

20. Kovacs CS, Kronenberg HM. Maternal-fetal calcium and bone metabolism during pregnancy, puerperium, and lactation. Endocr Rev 1997;18:832-72.

21. Winter EM, Ireland A, Butterfield NC, Haffner-Luntzer M, Horcajada MN, Veldhuis-Vlug AG, et al. Pregnancy and lactation, a challenge for the skeleton. Endocr Connect 2020;9:R143-R57.

22. Ryu SJ, Ryu DS, Kim JY, Park JY, Kim KH, Chin DK, et al. Changes in Bone Metabolism in Young Castrated Male Rats. Yonsei Med J 2016;57:1386-94.

23. Gomez-Gaviro MV, Balaban E, Bocancea D, Lorrio MT, Pompeiano M, Desco M, et al. Optimized CUBIC protocol for three-dimensional imaging of chicken embryos at single-cell resolution. Development 2017;144:2092-7.

24. Woo J, Jin B-H, Lee M, Lee EY, Moon H-S, Park J-Y, et al. Investigation of PRDM10 and PRDM13 Expression in Developing Mouse Embryos by an Optimized PACT-Based Embryo Clearing Method. International Journal of Molecular Sciences 2021;22.

25. Park JA, Kim KC. Expression patterns of PRDM10 during mouse embryonic development. BMB Rep 2010;43:29-33.

26. Sanghani-Kerai A, Osagie-Clouard L, Blunn G, Coathup M. The influence of age and osteoporosis on bone marrow stem cells from rats. Bone Joint Res 2018;7:289-97.

27. Courties A, Belle M, Senay S, Cambon-Binder A, Sautet A, Chedotal A, et al. Clearing method for 3-dimensional immunofluorescence of osteoarthritic subchondral human bone reveals peripheral cholinergic nerves.

연세대학교
YONSEI UNIVERSITY

Sci Rep 2020;10:8852.

28. Susaki EA, Tainaka K, Perrin D, Yukinaga H, Kuno A, Ueda HR. Advanced CUBIC protocols for whole-brain and whole-body clearing and imaging. Nat Protoc 2015;10:1709-27.

29. Murakami TC, Mano T, Saikawa S, Horiguchi SA, Shigeta D, Baba K, et al. A three-dimensional single-cell-resolution whole-brain atlas using CUBIC-X expansion microscopy and tissue clearing. Nat Neurosci 2018;21:625-37.

30. Susaki EA, Tainaka K, Perrin D, Kishino F, Tawara T, Watanabe TM, et al. Whole-brain imaging with single-cell resolution using chemical cocktails and computational analysis. Cell 2014;157:726-39.

31. Jing D, Yi Y, Luo W, Zhang S, Yuan Q, Wang J, et al. Tissue Clearing and Its Application to Bone and Dental Tissues. J Dent Res 2019;98:621-31.

32. Liu H, Zhu R, Liu C, Ma R, Wang L, Chen B, et al. Evaluation of Decalcification Techniques for Rat Femurs Using HE and Immunohistochemical Staining. Biomed Res Int 2017;2017:9050754.

33. Savi FM, Brierly GI, Baldwin J, Theodoropoulos C, Woodruff MA. Comparison of Different Decalcification Methods Using Rat Mandibles as a Model. J Histochem Cytochem 2017;65:705-22.

34. Ramirez T, Sacchini S, Paz Y, Rosales RS, Camara N, Andrada M, et al. Comparison of Methods for the Histological Evaluation of Odontocete Spiral Ganglion Cells. Animals (Basel) 2020;10.

35. Roberts BC, Giorgi M, Oliviero S, Wang N, Boudiffa M, Dall'Ara E. The longitudinal effects of ovariectomy on the morphometric, densitometric and mechanical properties in the murine tibia: A comparison between two mouse strains. Bone 2019;127:260-70.

36. Fog CK, Galli GG, Lund AH. PRDM proteins: important players in differentiation and disease. Bioessays 2012;34:50-60.

37. Sorrentino A, Federico A, Rienzo M, Gazzerro P, Bifulco M,

연세대학교
YONSEI UNIVERSITY

Ciccodicola A, et al. PR/SET Domain Family and Cancer: Novel Insights from the Cancer Genome Atlas. Int J Mol Sci 2018;19.

연세대학교
YONSEI UNIVERSITY

APPENDICES

International Journal of
Molecular Sciences

MDPI

Article

Investigation of PRDM10 and PRDM13 Expression in Developing Mouse Embryos by an Optimized PACT-Based Embryo Clearing Method

Jiwon Woo [1,2,3,4,†], Byung-Ho Jin [1,5,6,†], Mirae Lee [1,2,4], Eunice Yoojin Lee [7], Hyung-Seok Moon [4], Jeong-Yoon Park [1,2,6] and Yong-Eun Cho [1,2,6,*]

1 Department of Neurosurgery, The Spine and Spinal Cord Institute, Gangnam Severance Hospital, Yonsei University College of Medicine, Seoul 06273, Korea; jiwonflu@yuhs.ac (J.W.); bhjinccf@hanmail.net (B.-H.J.); alfo0103@naver.com (M.L.); spinepjy@yuhs.ac (J.-Y.P.)
2 Brain Korea 21 PLUS Project for Medical Science, Yonsei University, Seoul 03722, Korea
3 Biomedical Research Institute, Biohedron Therapeutics Co., Ltd., Seoul 06230, Korea
4 Biomedical Research Center, Gangnam Severance Hospital, Yonsei University College of Medicine, Seoul 06230, Korea; moonsir@yuhs.ac
5 Department of Neurosurgery, International ST Mary's Hospital, College of Medicine, Catholic Kwandong University, Incheon 22711, Korea
6 Department of Neurosurgery, College of Medicine, Yonsei University Graduate School, Seoul 03722, Korea
7 College of Physicians and Surgeons, Columbia University Vagelos, New York, NY 10032, USA; euniceyj133@gmail.com
* Correspondence: yecho@yuhs.ac; Tel.: +82-2-2019-3390
† These authors contributed equally to this work.

check for updates

Citation: Woo, J.; Jin, B.-H.; Lee, M.; Lee, E.Y.; Moon, H.-S.; Park, J.-Y.; Cho, Y.-E. Investigation of PRDM10 and PRDM13 Expression in Developing Mouse Embryos by an Optimized PACT-Based Embryo Clearing Method. *Int. J. Mol. Sci.* **2021**, *22*, 2892. https://doi.org/10.3390/ijms22062892

Academic Editor: Dawit Tesfaye

Received: 19 January 2021
Accepted: 8 March 2021
Published: 12 March 2021

Publisher's Note: MDPI stays neutral with regard to jurisdictional claims in published maps and institutional affiliations.

Copyright: © 2021 by the authors. Licensee MDPI, Basel, Switzerland. This article is an open access article distributed under the terms and conditions of the Creative Commons Attribution (CC BY) license (https://creativecommons.org/licenses/by/4.0/).

Abstract: Recent developments in tissue clearing methods have significantly advanced the three-dimensional analysis of biological structures in whole, intact tissue, providing a greater understanding of spatial relationships and biological circuits. Nonetheless, studies have reported issues with maintaining structural integrity and preventing tissue disintegration, limiting the wide application of these techniques to fragile tissues such as developing embryos. Here, we present an optimized passive tissue clearing technique (PACT)-based embryo clearing method, initial embedding PACT (IMPACT)-Basic, that improves tissue rigidity without compromising optical transparency. We also present IMPACT-Advance, which is specifically optimized for thin slices of mouse embryos past E13.5. We demonstrate proof-of-concept by investigating the expression of two relatively understudied PR domain (PRDM) proteins, PRDM10 and PRDM13, in intact cleared mouse embryos at various stages of development. We observed strong PRDM10 and PRDM13 expression in the developing nervous system and skeletal cartilage, suggesting a functional role for these proteins in these tissues throughout embryogenesis.

Keywords: transparent embryo; embryo clearing; passive clearing technique; IMPACT; PRDM10; PRDM13

1. Introduction

Significant recent advancements in the field of tissue clearing have allowed for the appreciation of molecular patterns and cellular circuits in various biological tissues in three-dimensional space. As opposed to traditional immunohistochemistry in frozen or paraffin sections, clear lipid-exchanged acrylamide-hybridized rigid imaging/immunostaining/in situ-hybridization-compatible tissue-hydrogel (CLARITY)-based methods enable the microscopic study of tissue architecture in intact whole tissues and organs [1,2]. We recently reported the development of novel passive tissue clearing techniques (PACTs), process-separated PACT (psPACT) and modified PACTs (mPACT and mPACT-A), which significantly reduced required tissue processing times while improving achieved optical transparency [3–5].

Figure A1. A paper in published. Woo J*, **Jin BH***, Lee M, Lee EY, Moon HS, Park JY, Cho YE. Investigation of PRDM10 and PRDM13 Expression in Developing Mouse Embryos by an Optimized PACT-Based Embryo Clearing Method. Int J Mol Sci. 2021 Mar 12;22(6):2892. (* Co-first author).

연세대학교
YONSEI UNIVERSITY

Investigation of bone metabolism in rodents by using an optimized PACT-based bone clearing technique

Authors: Byung-Ho Jin[1,2,3*], Jiwon Woo[1,4,5,6*], Mirae Lee[1,4,6], Seockmo Ku[7], Hyung Seok Moon[6], Seung Jun Ryu[3], Jeong Yoon Park[1,2,4], Sung Uk Kuh[1,2,6,8], and Yong Eun Cho[1,2,4¶]

Affiliations:

[1] The Spine and Spinal Cord Institute, Department of Neurosurgery, Gangnam Severance Hospital, Yonsei University College of Medicine, Seoul, 06273 Republic of Korea

[2] College of Medicine, Yonsei University Graduate School, Seoul, 03722 Republic of Korea

[3] Department of Neurosurgery, International ST Mary´s Hospital, College of Medicine, Catholic Kwandong University, Incheon, 22711 Republic of Korea

[4] Department of Neurosurgery, Graduate School of Medical Science, Brain Korea 21 Project, Yonsei University College of Medicine, Seoul, 03722 Republic of Korea

[5] Biomedical Research Institute, Biohedron Co., Ltd., Seoul, 06230 Republic of Korea

[6] Biomedical Research Center, Gangnam Severance Hospital, Seoul, 06230 Republic of Korea

[7] Fermentation Science Program, School of Agriculture, College of Basic and Applied Sciences, Middle Tennessee State University, Murfreesboro, TN, 37132, USA

[8] Department of Medical Device Engineering and Management, Yonsei University College of Medicine, Seoul, 03722 Republic of Korea

* Byung-Ho Jin & Jiwon Woo. These authors contributed equally.

Figure A2. A paper in prepared for submission.

Jin BH*, Woo J*, Lee M, Lee EY, Moon HS, Ryu SJ, Park JY, Kuh SU, Cho YE. Investigation of the Bone Metabolism Pattern in Rodent by using Optimized PACT-based Bone Clearing Technique. (* Co-first author).

연세대학교
YONSEI UNIVERSITY

ABSTRACT(IN KOREAN)

뼈 조직 투명화 기술을 이용한 골다공증의 뼈 대사에 영향을 미치는 생체인자의 영상화

<지도교수 조용은>

연세대학교 대학원 의학과

진병호

최근 PACT(Passive Clearing Technique)와 같은 조직 청소 방법의 발전으로 인해 온전한 조직 전체의 생물학적 구조를 3차원적으로 분석할 수 있게 되어 공간 관계와 생물학적 회로에 대한 더 큰 이해를 제공했다. 그럼에도 불구하고, 구조적 무결성을 유지하고 신속한 투명화로 조직 확장/수축을 방지하고 이러한 기술을 대퇴골 및 경골과 같은 경골 조직에 대한 적용에서 확장/수축을 방지하는 문제가 남아 있다. 여기서는 Calci-mPACT+ 및 20EDTA-mPACT+를 통합하여 광학 투명도를 감소하지 않으면서 뼈 조직 투명화 효율을 개선하는 최적화된 psPACT 기반 뼈 제거 방법인 Bone-mPACT+를 제시한다. 우리는 또한 확립된 조직 제거 방법을 사용하여 손쉬운 제거 및 이미징을 위해 가장 크고 단단한 쥐 뼈를 처리하도록 특별히 최적화된 추가 수정된 Bone-mPACT+ Advance 기법을 제시한다. 우리는 임신 중 모체 쥐 뼈와 고환 절제술 후 남성 골다공증 모델 백서의 뼈에서 내인성 형광과 RUNX2, OPG, RANKL 및 상대적으로 연구되지 않은 PRDM10 및 PRDM12의 발현을 조사하여 최적화된 방법론에 대한 개념 증명 결과를 제시한다. 골다공증 발달 동안 투명한 뼈에서 OPG, RANKL, PRDM10 및 PRDM12 발현에 대한 우리의 관찰은 대사 및 퇴행성 뼈 질환의 미래 기능 연구를 안내할 수 있는 이러한 유전자의 잠재적 역할을 제시한다.

핵심되는 말 : 투명한 뼈, 뼈 투명화, 수동형 조직 투명화 기술, Bone-mPACT+ 기법, 골다공증

연세대학교
YONSEI UNIVERSITY

PUBLICATION LIST

Woo J*, **Jin BH***, Lee M, Lee EY, Moon HS, Park JY, Cho YE. **Investigation of PRDM10 and PRDM13 Expression in Developing Mouse Embryos by an Optimized PACT-Based Embryo Clearing Method.** *Int J Mol Sci.* 2021 Mar 12;22(6):2892. doi: 10.3390/ijms22062892. PMID: 33809237; PMCID: PMC8000312. (* Co-first author).

Jin BH*, Woo J*, Lee M, Lee EY, Moon HS, Ryu SJ, Park JY, Kuh SU, Cho YE. **Investigation of the Bone Metabolism Pattern in Rodent by using Optimized PACT-based Bone Clearing Technique**. (* Co-first author).